

Review

A Review on Recent Advances and Future Trends of Transformerless Inverter Structures for Single-Phase Grid-Connected Photovoltaic Systems

Kamran Zeb ^{1,2} , Imran Khan ¹, Waqar Uddin ¹ , Muhammad Adil Khan ¹, P. Sathishkumar ¹, Tiago Davi Curi Busarello ³ , Iftikhar Ahmad ² and H. J. Kim ^{1,*}

¹ School of Electrical Engineering, Pusan National University, San 30, ChangJeon 2 Dong, Pusandaehak-ro 63 beon-gil 2, Geumjeong-gu, Busan 46241, Korea; kami_zeb@yahoo.com (K.Z.); imrankhan@pusan.ac.kr (I.K.); waqar_dir98@yahoo.com (W.U.); engradilee@gmail.com (M.A.K); sathishnano2013@gmail.com (P.S.)

² School of Electrical Engineering and Computer Science, National University of Sciences and Technology, Islamabad-44000, Pakistan; iftikhar.rana@seecs.edu.pk

³ School Department of Engineering Federal, University of Santa Catarina Blumenau, Rua João Pessoa 2750-89036-256, Brazil; tiago.busarello@ufsc.br

* Correspondence: heeje@pusan.ac.kr; Tel.: +82-010-3462-1990

Received: 6 July 2018; Accepted: 24 July 2018; Published: 28 July 2018



Abstract: The research significance of various scientific aspects of photovoltaic (PV) systems has increased over the past decade. Grid-tied inverters the vital elements for the effective interface of Renewable Energy Resources (RER) and utility in the distributed generation system. Currently, Single-Phase Transformerless Grid-Connected Photovoltaic (SPTG-CPV) inverters (1–10 kW) are undergoing further developments, with new designs, and interest of the solar market. In comparison to the transformer (TR) Galvanic Isolation (GI)-based inverters, its advantageous features are lower cost, lighter weight, smaller volume, higher efficiency, and less complexity. In this paper, a review of SPTG-CPV inverters has been carried out. The basic operational principles of all SPTG-CPV inverters are presented in details for positive, negative, and zero cycles. A comprehensive analysis of each topology has been deliberated. A comparative assessment is also performed based on weaknesses, strengths, component ratings, efficiency, total harmonic distortion (THD), semiconductor device losses, and leakage current of various SPTG-CPV inverters schemes. Typical PV inverter structures and control schemes for grid connected three-phase system and single-phase systems are also discussed, described, and reviewed. Comparison of various industrial grids-connected PV inverters is also performed. Loss analysis is also performed for various topologies at 1 kW. Selection of appropriate topologies for their particular application is thoroughly presented. Then, discussion and forthcoming progress are emphasized. Lastly, the conclusions are presented. More than 100 research publications on the topic of SPTG-CPV inverter topologies, configurations, and control schematics along with the recent developments are thoroughly reviewed and classified for quick reference.

Keywords: renewable energy resources; solar photovoltaic; single-phase grid-connected; transformerless inverter

1. Introduction

Long-term national strategies prove that the conventional power generation resources are unsustainable. In the last decade, extensive installation of renewable energy resources (RERs), i.e., hydropower, wind energy, solar photovoltaic (PV) energy, ocean energy, geothermal energy, biomass energy, tidal energy, and thermoelectric energy, has been enhanced for grid inter-connection [1–3]. Over

the past several years, solar PV energy installation is booming at a rapid rate and in some countries, it plays a vital role in electricity generation [4]. For instance, solar PV systems fulfill approximately 7.9% of annual electricity demands throughout 2014 in Italy. By the end of 2014, its installed capacity reached to 38.2 GW (mostly for residential purposes) [4–6]. In 2017, the installed capacity of solar PV and wind energies was 405 GW and 540 GW, respectively [5]. It is forecast that in the near future (2020) the installed capacity of solar PV (772 GW) will surpass wind energy (735 GW) [7].

The power converters play a key role in the integration of RER, including solar PV, in the grid [6,8]. Power semiconductor devices are associated with advancement [9], therefore, the power electronics part is accountable for efficient and reliable power conversion from inexhaustible, clean and pollution-free solar PV energy. That's why a large number of PV power converters for grids are advanced and commercialized [7,10–15]. In the grid-connected PV system, the popularity of inverters that converts DC power from the PV module into AC power for grid injection is increasing day by day. Usually a voltage source inverter (VSI) or current source inverter (CSI) in combination with a DC/DC converter is used for integration of PV systems into the grid. A sophisticated control structure is also required to achieve better performance and obtain the desired output from the system. In control mechanisms, an inverter plays an important role in controlling the injection of grid current. Hence, it maintains the DC link voltage value at the desired level and control the flow of both active and reactive power to the grid [9,15].

There is a significant variation of grid-connected PV systems from a few hundred Watts (small-scale DC modules) to hundreds of megawatts (large scale). In comparison to the transformer (TR) GI-based inverters its advantageous features are lower cost, lighter weight, smaller volume, higher efficiency, and less complexity. On the basis of leakage current reduction approaches these topologies are principally categorized as: GI with common mode voltage (CMV) clamping and without CMV clamping. By incorporating extra switches, the GI can be acquired either on AC side or DC side of full bridge (FB) or neutral point clamped (NPC) topology, due to the fact a lower number of switches in conduction path AC side decoupling offers high efficiency. As stated earlier, a large portion of residential applications consists of PV systems and these are expected to greatly spread in the near future. The technological development in the power electronics sector has brought high efficiency and large varieties of transformerless inverters into existence that are derived from the H-bridge inverter design. These derived inverter topologies have higher efficiencies and low EMI/CM (H5, HERIC). This review comprehensively reviews the development and control of transformerless topologies. The remainder of this survey is systematized as follows: a discussion about power converter technology for PV systems along with a categorization of transformerless inverter topologies are carried out in Section 2. H-bridge based inverter structures are investigated in Section 3. Section 4 scrutinizes the NPC-derived inverter technologies. Regarding transformerless PV inverters, a comparative and characteristic overview is presented in Section 5. Typical PV inverters structures and detail control structures for grid connected three-phase system and single-phase systems are explained in Section 6. Finally, Section 7 concludes this survey with a brief proposal for future work.

2. Power Converter Technology for PV Systems

Referring to progressing technologies to transfer to and organize the PV power in the grid, there are mainly five configuration concepts [1,10,16,17] available, as presented in Figure 1. According to the power rating and the output voltage of the PV panels, each configuration comprises a sequence of parallel strings of PV panels, followed and configured by DC-AC inverters and DC-DC converters (power electronics converters).

Typically, the power converters are classified into string inverters, multi-string inverters, central, and module level (AC module and DC module) inverters [10,11]. For solar power farms/plants configured as three-phase systems, the central and multi-string converters are widely utilized [18–20]. Comparatively, in residential applications configured as a single-phase system, string and module converters are intensively adopted [21,22]. Though the configuration of the power converters is

different, the power converters have the same major functions, including islanding detection and protection, reactive power control, grid code compliance, synchronization, power transfer and DC to AC conversion, and PV power maximization [10,16–28]. Advanced and intelligent controls are required for effective incorporation of these functionalities and to fulfill customized demands. Additionally, the PV integration can be enhanced by forecasting, monitoring, and communication technology [18–22].

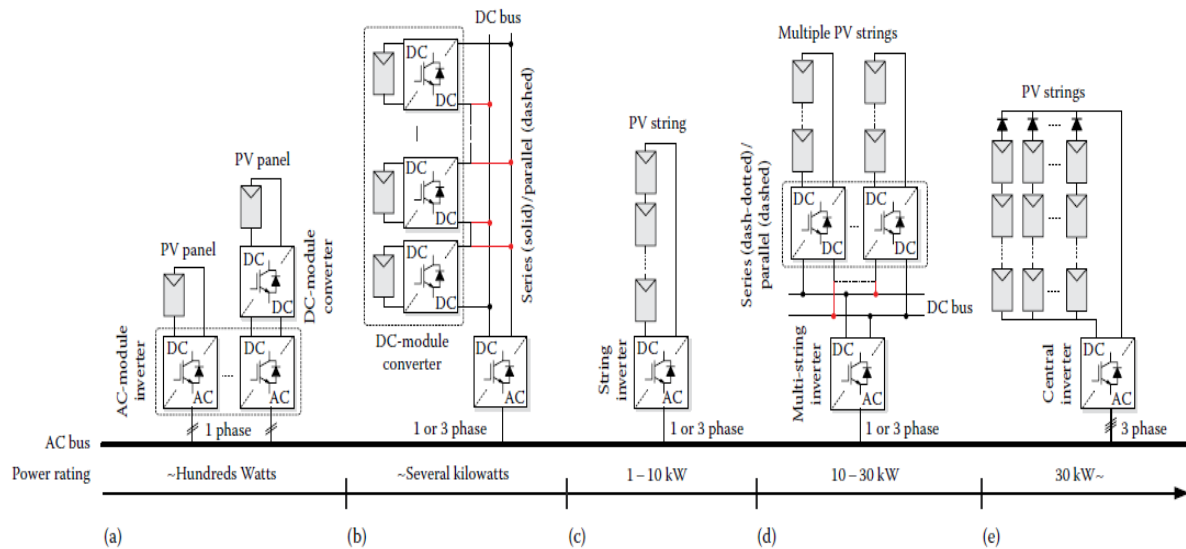


Figure 1. Power converter technology for PV system: (a) Residential/small systems, (b) residential/small systems, (c) residential, (d) residential /commercial, and (e) utility-scale/commercial PV applications [29].

String inverters, multistring inverters, and modular concept inverters are mostly used in single-phase PV system applications as depicted in Figure 1. In all these inverters the GI for safety is an important problem to be resolved. Conventionally, isolation is provided by a low frequency isolation transformer or a high frequency isolation transformer. The low frequency isolation transformer is used on the grid side while high frequency isolation transformers are used between the power electronics converters. With an overall efficiency of 93%–95%, both the abovementioned grid-connected technologies are commercially available, constituted mainly by bulky transformers [30]. A large number of transformerless PV inverters have been developed [5,7,10] and are progressing daily, in order to enhance the overall efficiency.

Currently, several manufacturing companies, i.e., Ingeteam, REFU, SMA, Conergy, Danfos Solar, and Sunways are in the market working on transformerless PV inverters. These inverters have European efficiency (>97%) and offer maximum efficiencies of up to 98%. The topology development for the transformerless inverter is based on the following main converter families:

- (a) H-bridge or full-bridge (BP)
- (b) NPC

Based on these main families, most relevant derived transformerless topologies are discussed and described in this survey. In some structures, a boost DC-DC converter is essential, which is why the level of diversity is high.

Classification of Transformerless Inverter Topologies

Transformers inverters are principally categorized on the basis of reduction in leakage current as: GI with CMV clamping and without CMV clamping. By incorporating extra switches, the GI can be acquired either on DC side or the AC side of H-bridge or NPC topology. There are low number of

switches in the conductive path, therefore, the AC side decoupling offers high efficiency. Additionally, leakage currents cannot be minimized merely on GI due to stray capacitances formed between the resonant circuit effect and switch terminals to heat sinks. The leakage current is completely eliminated through some topologies by fixing the CMV to half of the DC-link using clamping method. Figure 2 presents a categorization of transformerless inverter topologies [10,25–28,30–42].

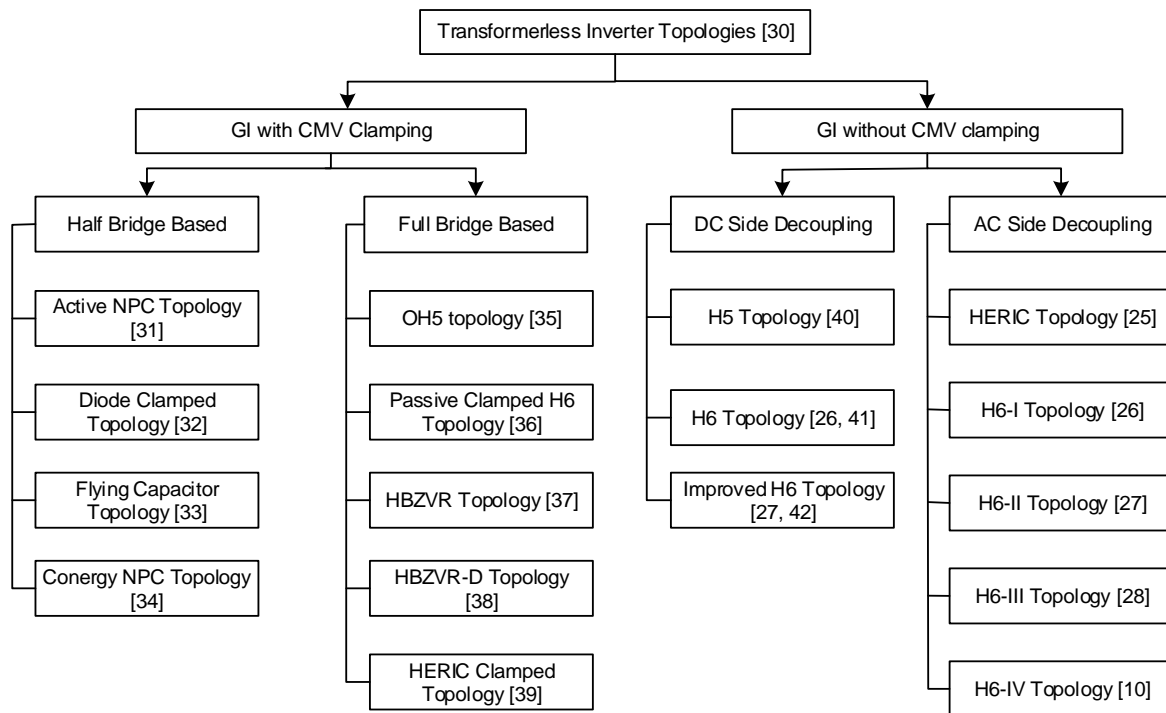


Figure 2. Transformerless inverter topologies: A classification overview.

3. H-bridge Based Inverter Structures

In 1965, McMurray first developed the FB or H-bridge inverter family [29]. In power converter technology, the FB is one of the important developments. The force-commuted semiconductor devices, also called thyristors was first effectively utilized by this structure. This topology can be implemented with one switching leg (in half bridge form) or with two switching legs (in FB form), they can be utilized for both DC-AC and DC-DC conversion, so it's also a versatile topology. The basic structure of FB is presented in Figure 3.

We consider a single stage inverter in our analysis for easiness, in single stage inverter MPPT DC-DC converter is not required. In case of half-bridge (HB) capacitive divider central point is grounded to limit the leakage current to guarantee the regulation of CMV. This leakage current flows through the parasitic capacitance of solar PV modules [42]. Low cost is the distinguishing feature, but the output voltage waveforms with two levels, switches must withstand high potential and highly distorted output current results in high electromagnetic interference (EMI) emissions and is considered a drawback of this topology [43]. The multi-level HB suggested by Calais et al. [44] in which he explored the concerns such as stimulus of the PV array Earth resistance and system power rating, stress and component count for SPG-C PV structures. For grid-connected PV system, HB is cascaded in five levels, as suggested in [45]. For PV application, extensively unipolar PWM modulation scheme is utilized in which CMV ($V_{dc}/2$) with high frequency is connected to the PV panels. The presence of non-negligible leakage current is considered a drawback in this technique due to the parasitic capacitance of PV panel [46]. To eliminate leakage current, the bipolar PWM modulation scheme is used [47,48].

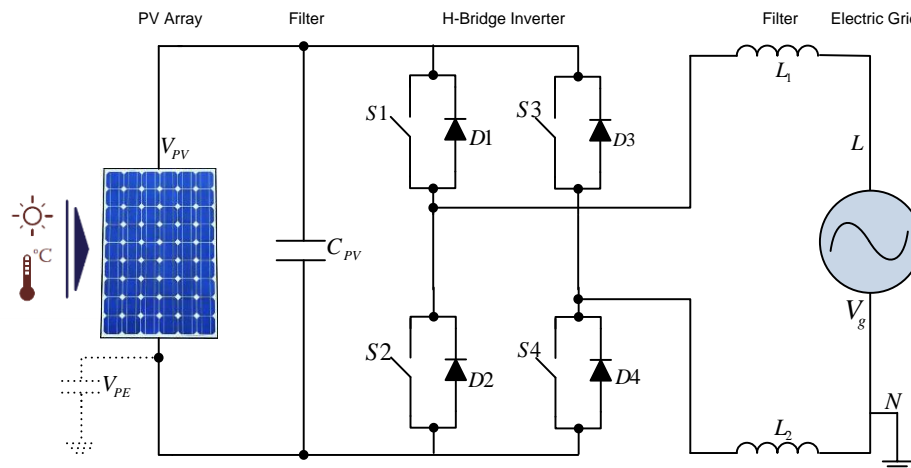


Figure 3. Basic structure of FB inverter [43].

3.1. Modulation Strategies

The basic modulation strategies for inverter structure are:

1. Two-level modulation
2. Three-level modulation
3. Hybrid modulation

3.1.1. Two Level Modulation

Two level modulation is also known as bipolar (BP) modulation. In the two-level modulation, the diagonal switches are turned on as S1 with S4 or S2 with S3, respectively. The AC output voltage can be obtained from these positive and negative output currents of the converter as depicted in Figure 4a,b [29,49]. This converter is based on the following features:

- The diagonal switches are synchronously switched on i.e., S1 with S4 or S2 with S3 at high frequency.
- Zero voltage state at the output is not possible.

I. Advantages

The EMI and leakage current is very low as voltage to ground V_{PE} has no switching frequency component, while only the grid frequency component is present [49].

II. Disadvantages

The disadvantages of this topology are: (a) the efficiency is low, around 95%, because of simultaneously switching of the two switches at every period, the output filter core losses are higher along with exchange of reactive power between $L_{1\leftrightarrow 2}$ and C_{PV} during freewheeling. (b) The filtering requirement is higher as in the current, the switching ripple is equivalent to $1 \times$ switching frequency. (c) Due to bipolar voltage variation, i.e., $(+V_{PV} \rightarrow -V_{PV} \rightarrow +V_{PV})$ the core losses are higher.

III. Analysis

Because of the decreased efficiency, the two-level modulation-based FB is inappropriate for use in transformerless PV systems although it has low leakage current.

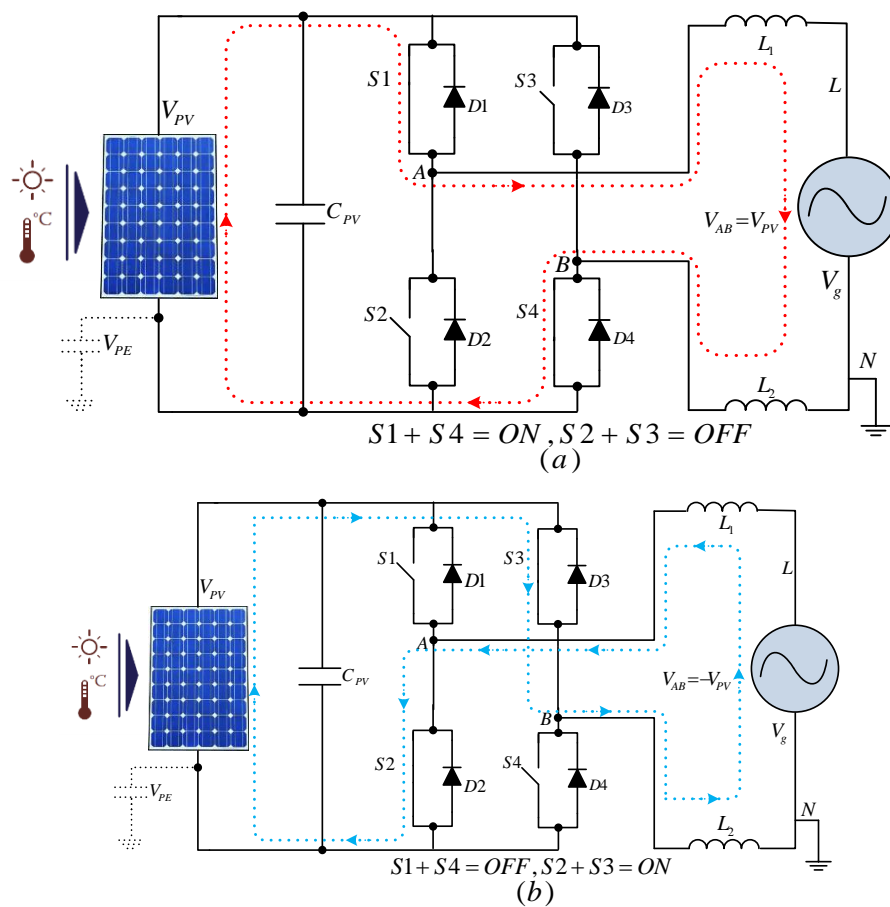


Figure 4. Two-level modulation scheme for FB in case of (a) positive cycle and (b) negative cycle [29,30].

3.1.2. Three-Level Modulation

Three-level modulation is also known as unipolar (UP) modulation. In this modulation, the switching signal of each leg is achieved according to its respective reference signal. For the positive and negative output currents, the AC voltage can be produced as presented in Figure 5 [29,49]. This converter is based on the following features:

- Switching of leg, A and leg B at high-frequency with reflected sinusoidal reference.
- Voltage state with zero output is probable: when S1, S3 or S2, S4 are ON.

I. Advantages

Three-level modulation schemes have the following advantages: (a) The filtering requirement is lower as in the output current, the switching ripple is equivalent to $1 \times$ switching frequency. (b) Due to unipolar voltage variation i.e., $(0 \rightarrow +V_{PV} \rightarrow 0 \rightarrow -V_{PV} \rightarrow 0)$ the core losses are lower. (c) Because of reduced losses during zero voltage states, its efficiency is higher, up to 98%.

II. Disadvantages:

The EMI and leakage current is very high as V_{PE} has no switching frequency component.

III. Analysis

Because of the large frequency content of the V_{PE} the three-level modulation-based FB is not appropriate for use in transformerless PV systems although it has high efficiency and low filtering requirements.

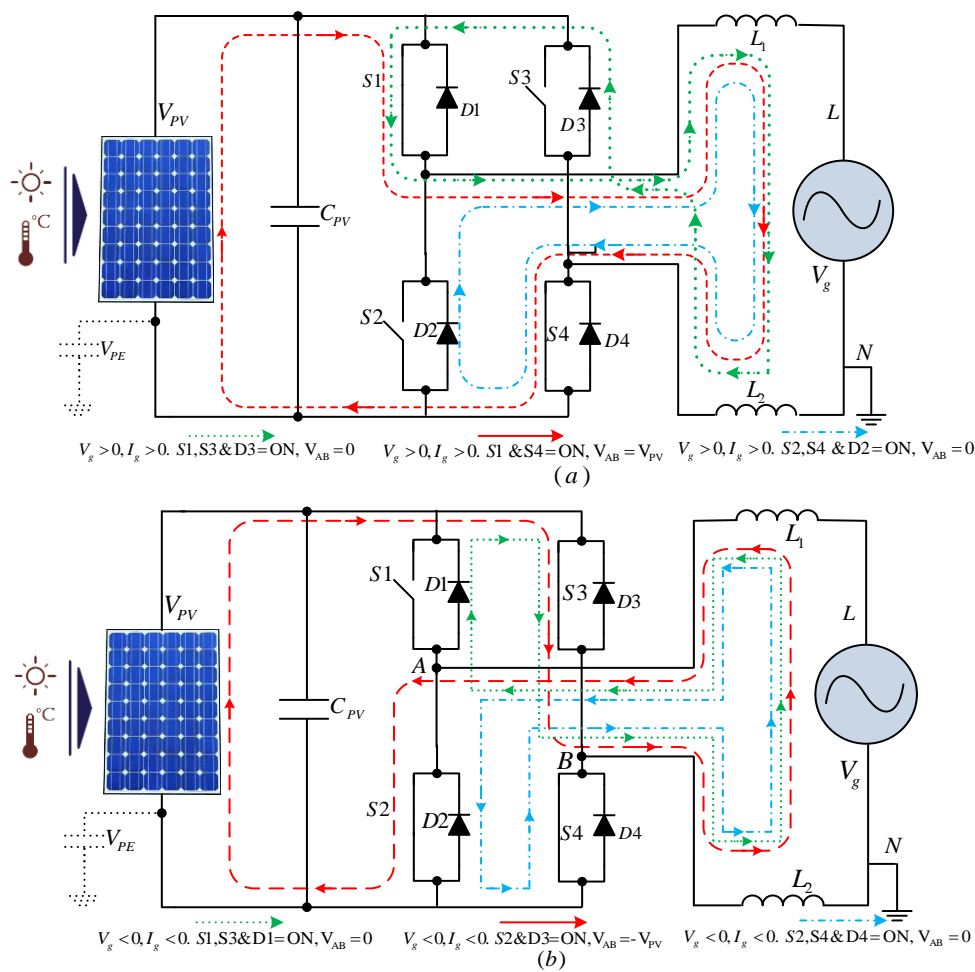


Figure 5. Three-level modulation scheme for FB in case of (a) positive cycle and (b) negative cycle [29,30].

3.1.3. Hybrid Modulation

According to the hybrid modulation (HM) concept, one leg is turned on at a higher frequency and the other leg is turned on at grid frequency [50,51]. For the positive and negative output currents, the AC voltage can be produced as described in Figure 6. This converter is centered on the subsequent features:

- At high PWM frequency, leg A is turned on while leg B is turned on at grid low frequency.
- Voltage state with two zero output is possible: when S_1, S_2 or S_3, S_4 are ON.

I. Advantages:

Its advantages are: (a) Due to unipolar voltage variation, i.e., $(0 \rightarrow +V_{PV} \rightarrow 0 \rightarrow -V_{PV} \rightarrow 0)$ the core losses are lower. (b) Its efficiency is higher, up to 98% because of no reactive power transfer between C_{PV} and $L_{1(2)}$ during zero voltage and one leg low frequency switching.

II. Disadvantages:

This topology has the following disadvantages: (a) V_{PE} has square wave variation at grid frequency, leading to high leakage current peaks and large EMI filtering requirements. (b) The filtering requirement is higher (in the output no artificial frequency increase) as in the current, the switching ripple is equivalent to $1 \times$ switching frequency. (c) For two quadrant operation, this modulation only

works [30]. In addition, for the first quadrant the triggering angle is $0 < \alpha < 90^\circ$ and for two quadrant the triggering angle is $90^\circ < \alpha < 180^\circ$

III. Analysis:

Because of the square-wave variation of the V_{PE} the HM-based, FB is unsuitable for use in transformerless PV systems although it has high efficiency.

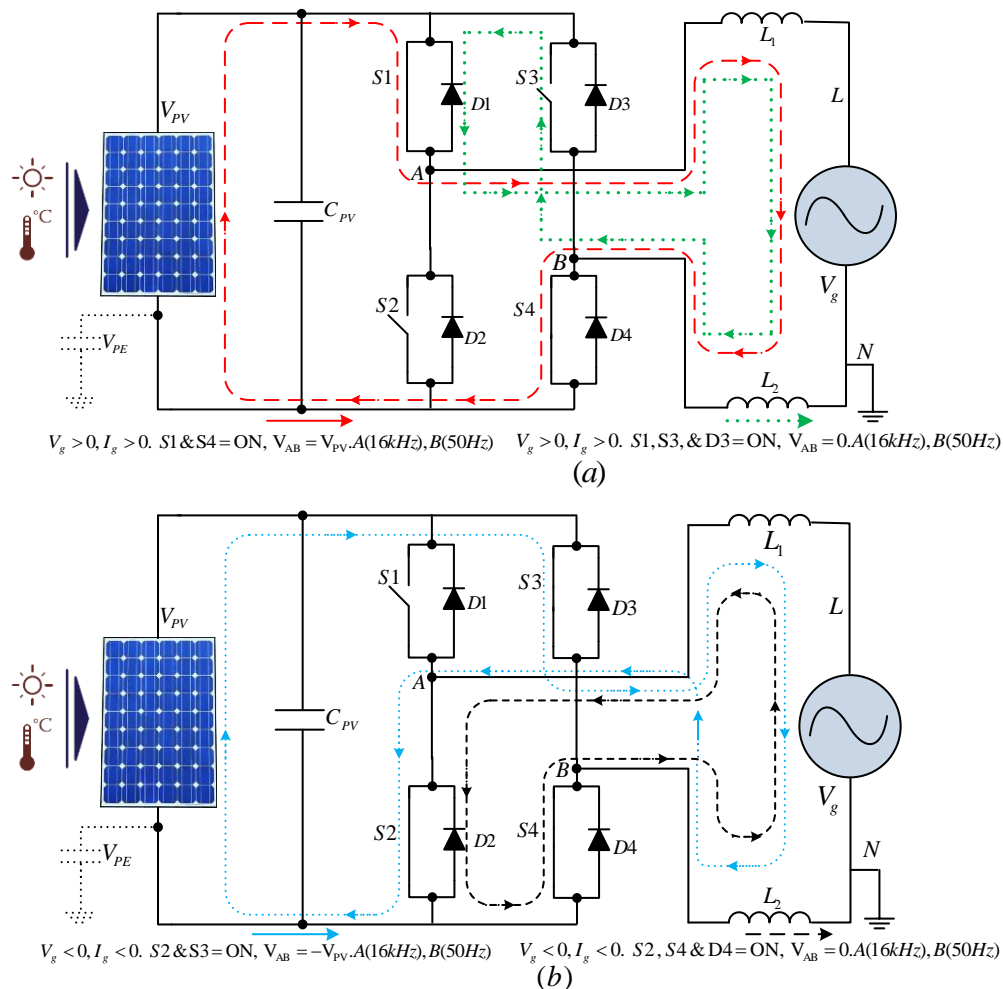


Figure 6. Hybrid modulation scheme for FB in case of (a) positive cycle and (b) negative cycle [29,30].

3.2. H5 Inverter (SMA)

A new inverter topology called H5 was patented by SMA in 2005 [52]. As specified by its name, it is a modified H-bridge, where in the DC-link (positive bus) an extra fifth switch is added, as presented in Figure 7. The extra switch has the following two vital functions: (a)The efficiency is increased as no exchange of reactive power between C_{PV} and $L_{1(2)}$ during zero voltage occurs and (b) the high frequency contents of V_{PE} is eliminated by detaching the power grid from the PV modules during zero voltage state [31].

Figure 8 presents the generation of AC currents for the positive and negative switching states. Modeling output filter and advancing switching frequency in the H5 topology of the PV inverter, has been illustrated in [53] by using power devices based on SiC. The proposed design shows the dominance of H5 topology based on enhanced SiC, correlating silicon (Si)-based counterparts and non-optimized with respect to energy production. This converter is based on the succeeding features [46,54,55].

- Voltage states with two zero output are possible, i.e., when S5 OFF and S4 (S2) are ON.
- S1 and S3 are switched at grid frequency and S2, S4, and S5 are switched at high frequency.

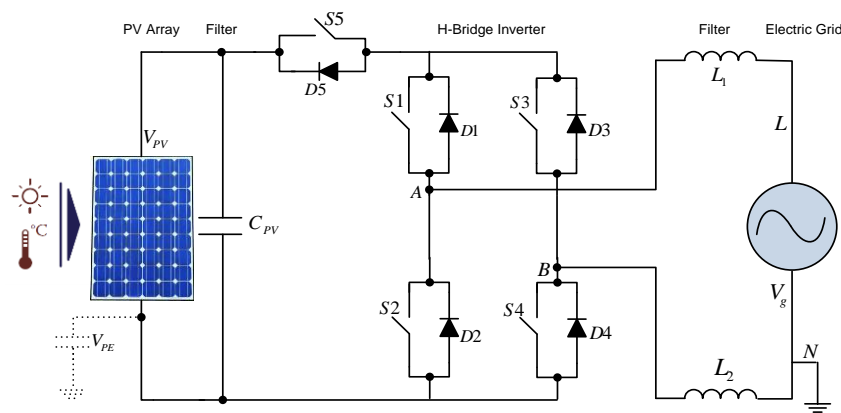


Figure 7. Schematic diagram of H5 (SMA) Inverter [43,56].

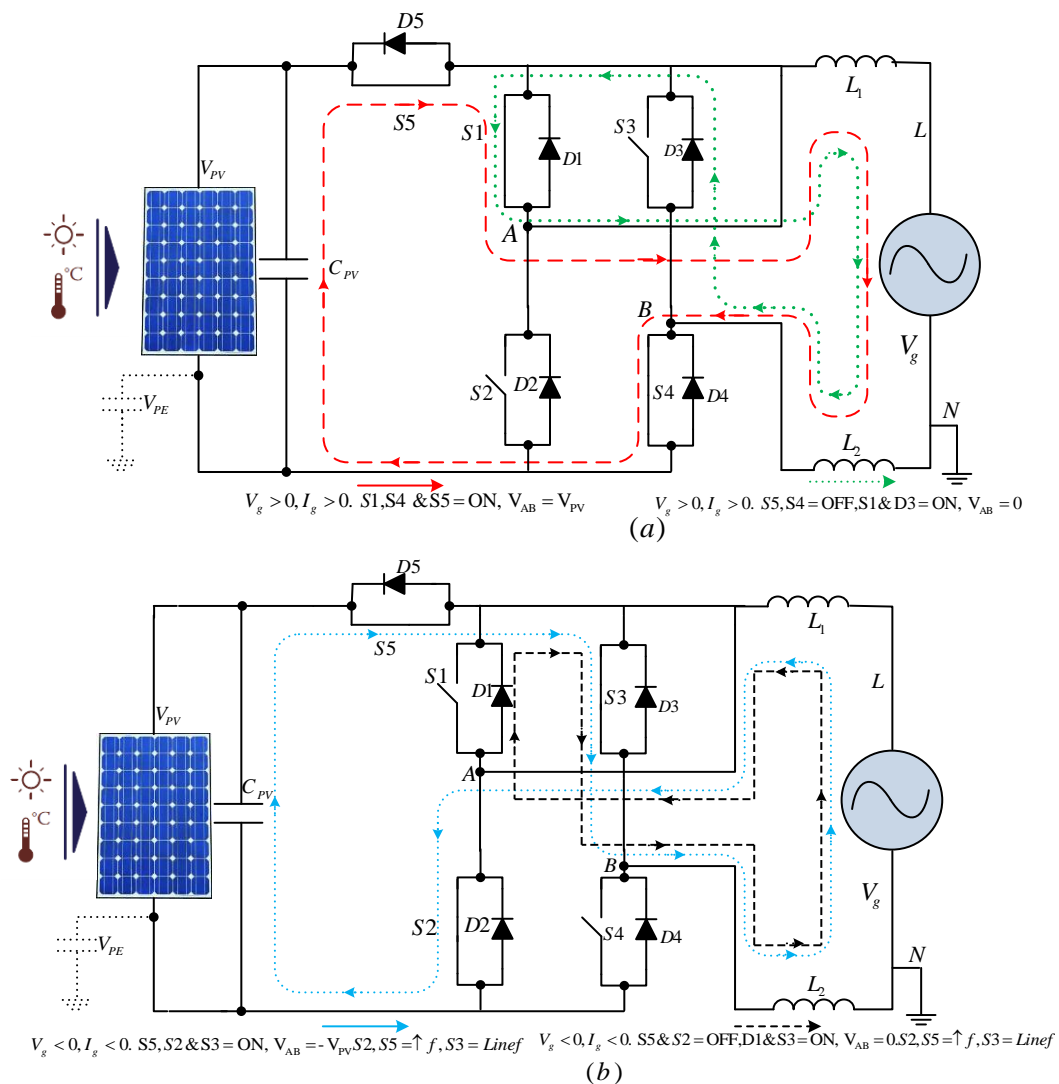


Figure 8. Switching positions of H5 (SMA) in case of (a) positive cycle and (b) negative cycle [29,30].

I. Advantages:

The H5 inverter advantages are: (a) The core losses are lower due to unipolar voltage variation i.e., $(0 \rightarrow +V_{PV} \rightarrow 0 \rightarrow -V_{PV} \rightarrow 0)$, (b) because of no exchange of reactive power between C_{PV} and $L_{1(2)}$ during zero voltage and in one leg, lower frequency switching, its efficiency is higher up to 98%, and (c) The EMI filtering requirement and the leakage current peaks is lower as V_{PE} has only grid frequency component [30].

II. Disadvantages:

Its disadvantages are: (a) The conduction losses are higher as the conducting switches are three during the active vector, but the overall high efficiency is not affected. (b) Addition of one extra switch.

III. Analysis:

The advantageous features of FB with hybrid modulation technique is combined in the H5 topology. Utilizing the extra switch, the high-frequency component of V_{PE} is eliminated by isolating the grid from the PV panels during zero voltage state situations. This scheme is very appropriate for utilization in transformerless PV system due its high efficient nature, lower EMI, and low filtering requirement at the output. Currently, it is commercialized by SMA in the SunnyBoy 4000/5000 TL series, with a maximum efficiency of 98% (Photon International, October 2007) and European efficiency higher than 97.7% [30].

3.3. HERIC Inverter (Sunways)

A new inverter topology called HERIC was patented by Sunways in 2006. The HERIC is also a highly reliable and efficient inverter approach. As presented in Figure 9, using two back to back connected insulated gate bipolar transistor (IGBT) a bypass leg is added to the AC side [57]. The AC bypass is used to provif4 the same fundamental functions as in the H5 topology with the extra fifth switch has. The efficiency is improved as no exchange of reactive power between C_{PV} and $L_{1(2)}$ during zero voltage occurs. The high-frequency component of V_{PE} is eliminated by isolating the grid from PV panels during zero voltage state [29].

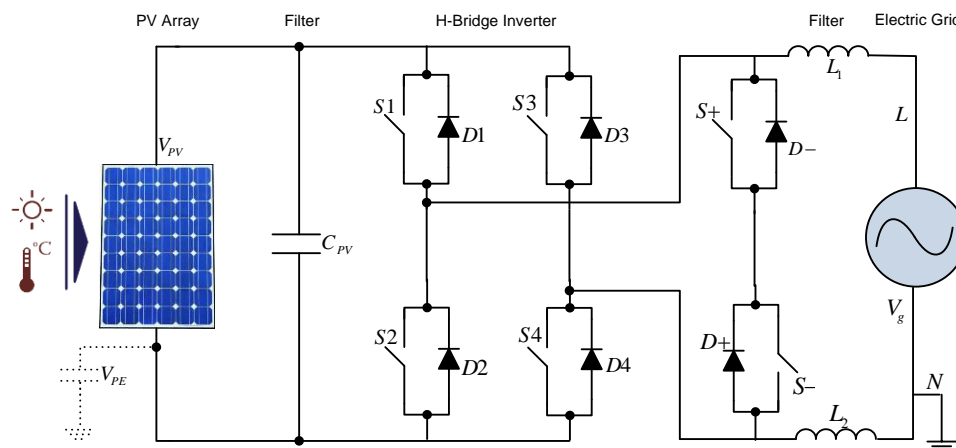


Figure 9. Schematic diagram of the Sunways HERIC Inverter [43,56].

Based on SPTG-CPV in parallel operation of HERIC topology with joint AC bus and DC bus, edges in improving the performance and accuracy of the PV generation system with DC module category expressed in [58,59]. The authors in [60], examined the capability of PV inverter based on the Low voltage ride-through (LVRT) potential of HERIC topology under grid support services and grid faults of PV systems.

Figure 10 presents the generation of AC currents for the positive and negative switching states. This converter is established based on the following features: (a) voltage states with two zero output is possible i.e., when S_+ ON and S_- are ON (in case for off state of the bridge), (b) S_+ (S_-) are turned on at grid frequency and S_1-S_4 or S_2-S_3 are turned on at high frequency.

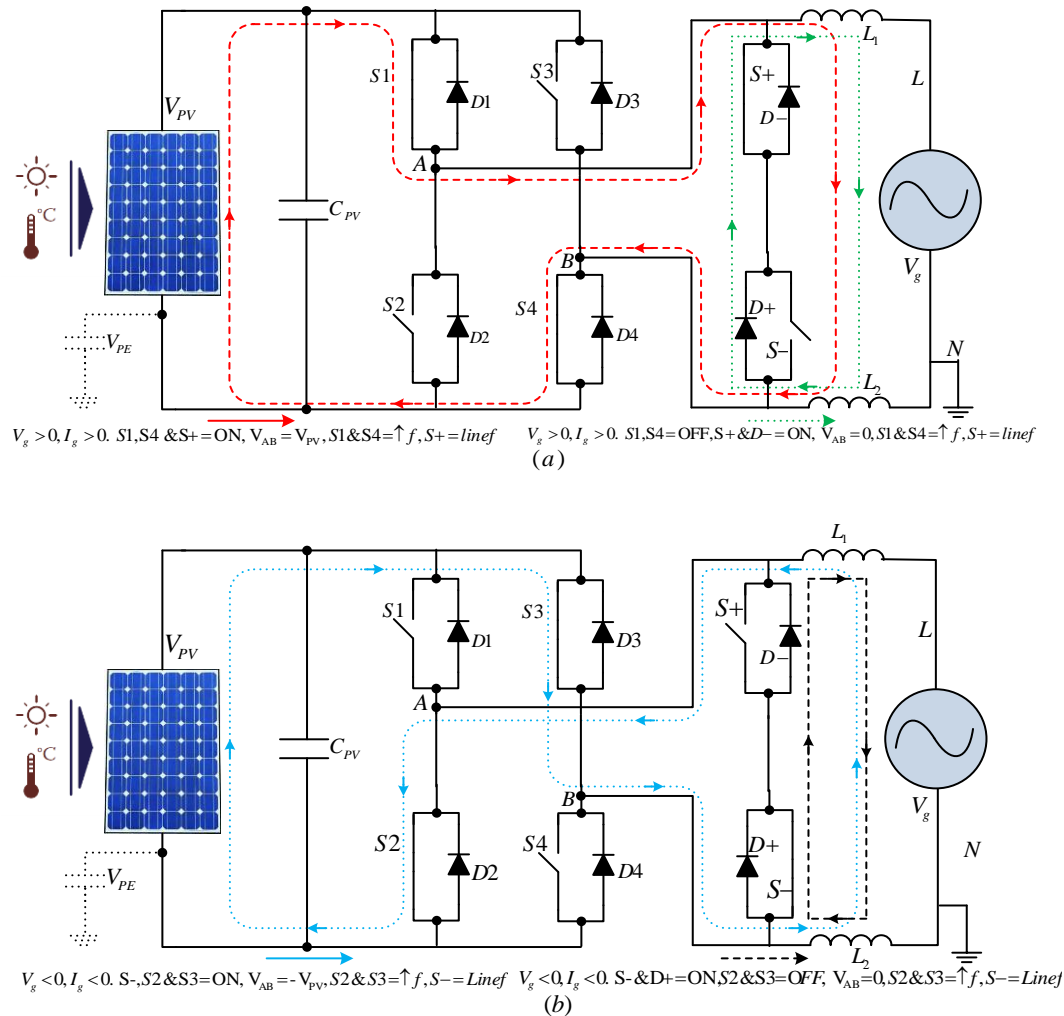


Figure 10. Switching states of the Sunways HERIC concept in case of: (a) positive cycle and (b) negative cycle [29,30].

I. Advantages

The HERIC topology has the following advantages: (a) the core losses are lower due to unipolar voltage variation i.e., $(0 \rightarrow +V_{PV} \rightarrow 0 \rightarrow -V_{PV} \rightarrow 0)$, (b) because there is no exchange of reactive power between C_{PV} and $L_{1(2)}$ during zero voltage and in one leg lower frequency switching, its efficiency is higher, up to 97%, and (c) The EMI filtering requirement and the leakage current peaks is lower as V_{PE} has no switching frequency component and only grid frequency component is present [29].

II. Disadvantages

Addition of two extra switches.

III. Analysis

The efficiency of the HERIC topology is increased by adding a zero-voltage level. This level is achieved with the help of AC bypass to the performance of FB with BP modulation technique. Due to

the high efficiency, low filtering requirements, and low EMI, for practical use in transformerless PV systems, this topology is thus very appropriate. Currently, Sunways commercializes a series called the AT series (2.7-5 kW), with a maximum efficiency of 95.6% (Photon International, July 2008) and a European efficiency of 95% [56].

As during the zero-voltage switching the decoupling of the grid from the PV generator on the DC side and AC side occurs, therefore both H5 and HERIC are quite similar in behavior. HERIC has only two switches conducting at the same time, while H5 has three. Additionally, of both switches, one switches at the grid frequency and two switches at high frequency.

3.4. REFU Inverter

A modification of the classical H-bridge design by REFU Solar gives a new layout patented in 2007. This topology usually consists of a by-passable DC-DC converter and a HB within the AC side bypass as presented in Figure 11 [61]. The same two vital functions of HERIC topology are provided by an AC bypass. i.e., The efficiency is improved as no exchange of reactive power between C_{PV} and $L_{1(2)}$ during zero voltage happens and removes the high-frequency content of V_{PE} , by detaching grid from the PV modules during zero voltage state [43].

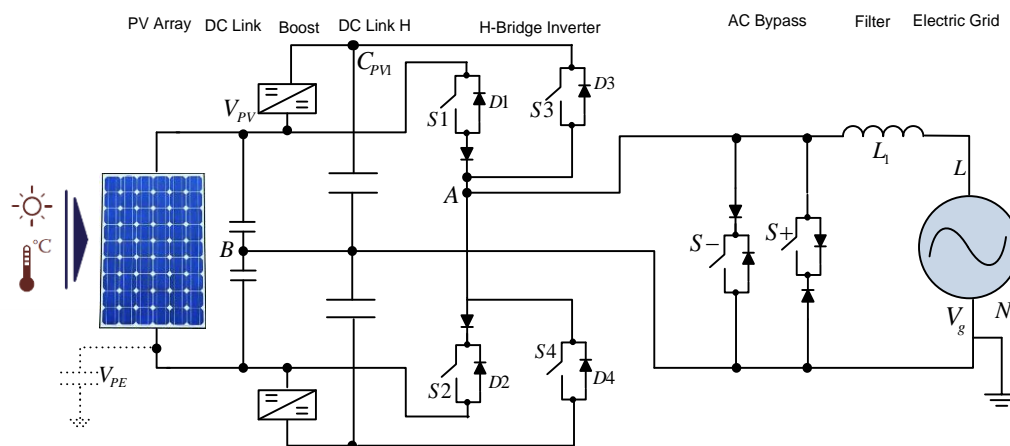


Figure 11. Schematic diagram of the REFU inverter [43,56].

In comparison to HERIC the AC bypass is implemented differently, e.g. standard IGBT module-based unidirectional switches are used, a series diode with IGBT is used to cancel the freewheeling path. In this topology, when the grid voltage is greater than the input DC voltage, only the boost converter is activated. Modulation techniques comprising double frequency PWM along with unipolar PWM are applied in H6 topology. Inductive current passing four active switches cause large conductive losses which are a disadvantage in this topology [39,56,62]. Using H6 topology replacing low efficient IGBTs with MOSFET was suggested [63]. Figure 12 presents the generation of AC currents for the positive and negative switching states. This converter is established based on the following features, e.g., (a) when boost is not needed: $V_{PV} > |V_g|$, then S1 (S2) are turned on at high frequency, (b) when boost is permitted: $V_{PV} < |V_g|$, then S3 (S4) are turned on at high frequency, (c) based on voltage polarity, S+ (S-) are switched at grid frequency [30].

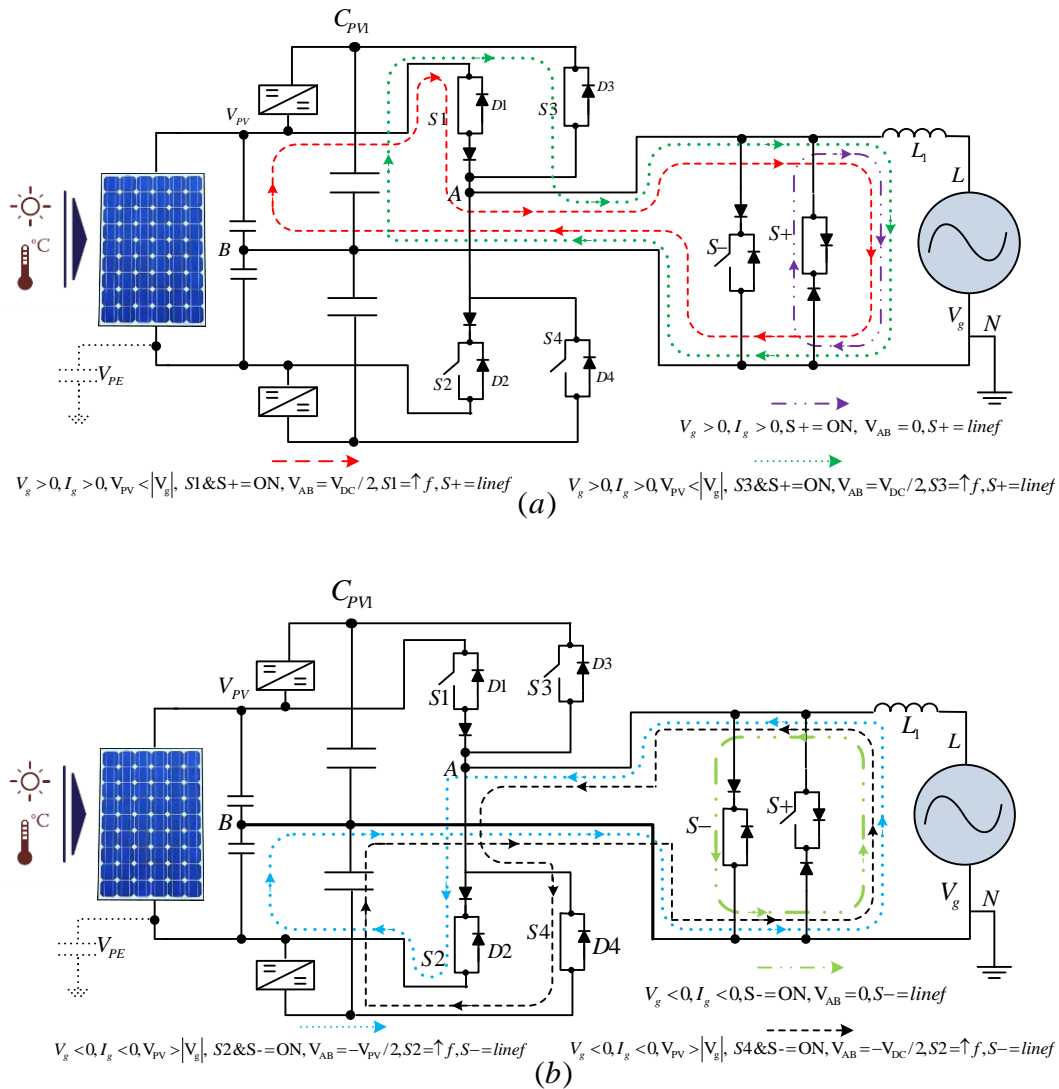


Figure 12. Switching positions of REFU (RefuSol) in case of (a) positive cycle and (b) negative cycle [29,30].

I. Advantages

The advantageous features of REFU are (a) the core losses are lower due to unipolar voltage variation i.e., $(0 \rightarrow +V_{PV} \rightarrow 0 \rightarrow -V_{PV} \rightarrow 0)$, (b) because of no exchange of reactive power between C_{PV} and $L_{1(2)}$ during zero voltage and in one leg lower frequency switching and boost only when necessary, its efficiency is higher up to 98%; (c) the EMI filtering requirement and the leakage current peaks is lower as V_{PE} has no switching frequency component and only grid frequency component is present [62].

II. Disadvantages

The following disadvantages are noted for REFU i.e.,: (a) addition of two more switches, although switched at a lower frequency and (b) dual DC voltage is needed.

III. Analysis

The REFU topology increases the efficiency with minimum losses by including the zero-voltage level with the help of an AC bypass to the performance of HB. Due to the high efficiency, low filtering requirements, and low EMI the REFU topology is more appropriate for use in transformerless PV

systems. Currently it is commercialized in the series called RefuSol (11/15 kW), with maximum efficiency of 98% (Photon International, September 2008) and a European efficiency of 97.5% [56].

3.5. FB-DCBP (Ingeteam) Inverter

The modification of the classical H-bridge by Ingeteam [64] gives a FB inverter with DC bypass (FB-DCBP) under a pending patent and described in [65]. This topology usually consists of a conventional H-bridge with the addition of two extra switches in the DC link and for clamping the output to the ground two extra diodes are coupled at the middle point of the DC bus as presented in Figure 13. In contrast to H5 or HERIC where the zero voltage is fluctuating, the zero-voltage grounding is ensured by the clamping diodes and the panels is separated from the grid by DC switches during zero voltage states. During zero voltage because of interruption of reactive power exchange between $C_{PV1(2)}$ and $L_{1(2)}$ leads to high efficiency and low leakage current, essentially “jump-free” V_{PE} solution is ensured by both. Figure 14 presents the generation of AC currents for the positive and negative switching states. The main function of FB-DCBP topology is as follows:

- The switches S_1 (S_2) or S_4 (S_3) are turned on at grid frequency while the switching frequency of S_5 and S_6 are high.
- Zero voltage at the output is attained by turning the DC bypass switches (S_5 & S_6) OFF. The current divides into two ways, When S_5 , S_6 are turned OFF and S_2 , S_3 are turned ON i.e., (a) The freewheeling diode (D_2) of S_2 and S_4 , and (b) S_1 and the freewheeling diode (D_3) of S_3 . Consequently, no switching losses appear as S_2 and S_3 are turned ON with no current. The current path during zero voltage state for negative grid current will be S_2 - D_4 or S_3 - D_1 , while for positive grid currents will be S_1 - D_3 or S_4 - D_2 . To the half of the DC-link voltage, for clamping the bypass switches $D+$ and $D-$ are used [10].

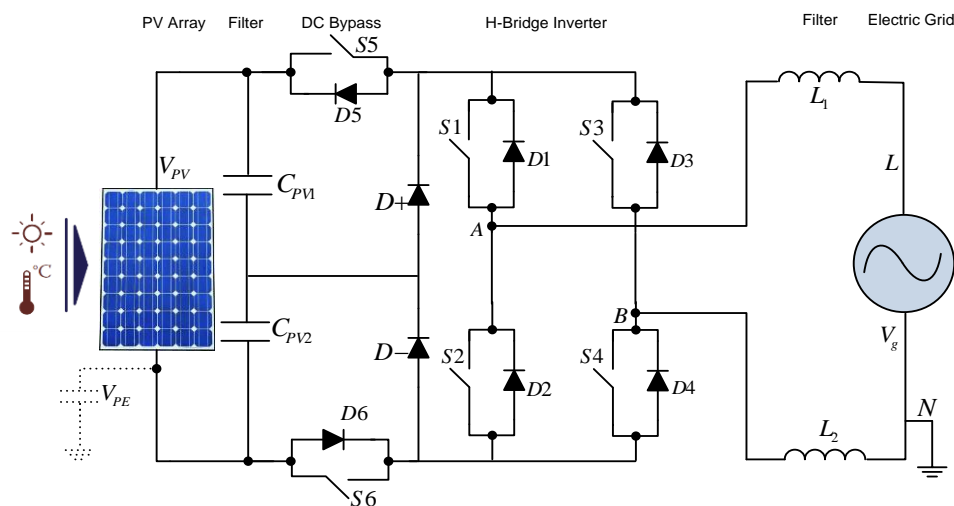


Figure 13. Schematic diagram of the Ingeteam FB-DCBP inverter [43,56].

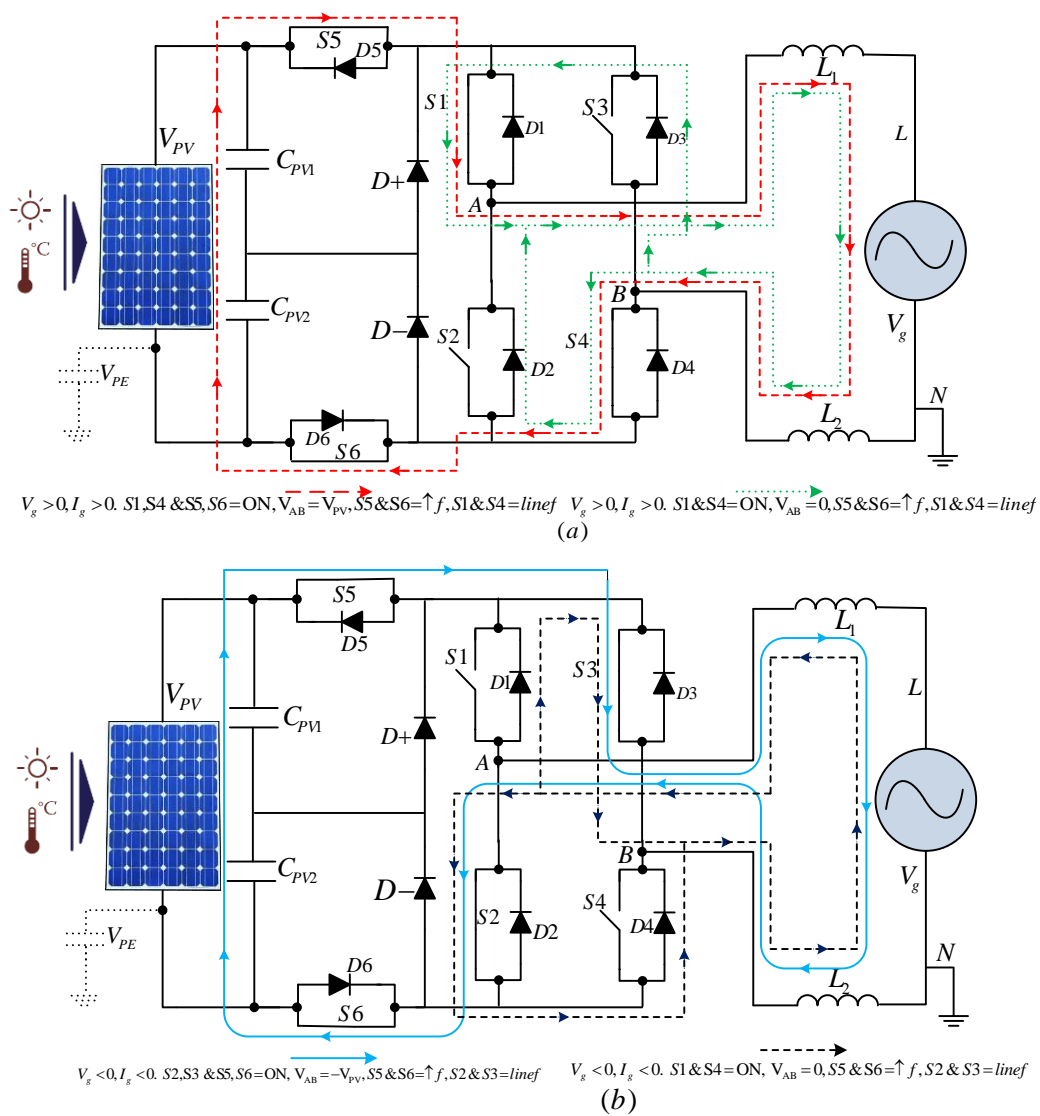


Figure 14. Switching positions of the Ingeteam FB-DCBP in case of: (a) positive cycle and (b) negative cycle [43,56].

I. Advantages

The beneficial features of FB-DCBP are: (a) the core losses are lower due to unipolar voltage variation i.e., $(0 \rightarrow +V_{PE} \rightarrow 0 \rightarrow -V_{PE} \rightarrow 0)$; (b) the DC bypass switches has the half of rating of DC voltage; (c) because of the low voltage rating of S5 and S6, a lower switching frequency in the FB, and no exchange of reactive power between C_{PV} and $L_{1(2)}$ during no voltage, its efficiency is higher up; (d) the EMI filtering requirement and the leakage current peaks is lower as V_{PE} has no switching frequency component and only grid frequency component is present [56].

II. Disadvantages

The negative features of FB-DCBP are: (a) addition of two extra diodes and two more switches; (b) without influencing the total high efficiency, the conduction losses are higher due to the fact four switches are conducting during the active vector.

III. Analysis

Due to low EMI, Low filtering requirement and high efficiency, the Ingeteam FB-DCBP topology is therefore very appropriate for practice in transformerless PV system. Currently, the series called Sun TL series (2.5/3.6/6 kW), is commercialized by Ingeteam in the Ingecon, with an ultimate efficiency of 96.5% (Photon International, Aug. 2007) and a European efficiency of 95.1% [64].

3.6. Full-Bridge Zero Voltage Rectifier-(FB-ZVR) Inverter

The other modification of the classical H-bridge is known as FB-ZVR [56], as presented in Figure 15. The derivation of this topology is based on the HERIC topology, using a diode clamp to the DC midpoint and one switch (S_5) and a diode bridge, the bidirectional grid short-circuiting switch is executed. By turning S_5 on and turning the FB off the zero voltage is achieved.

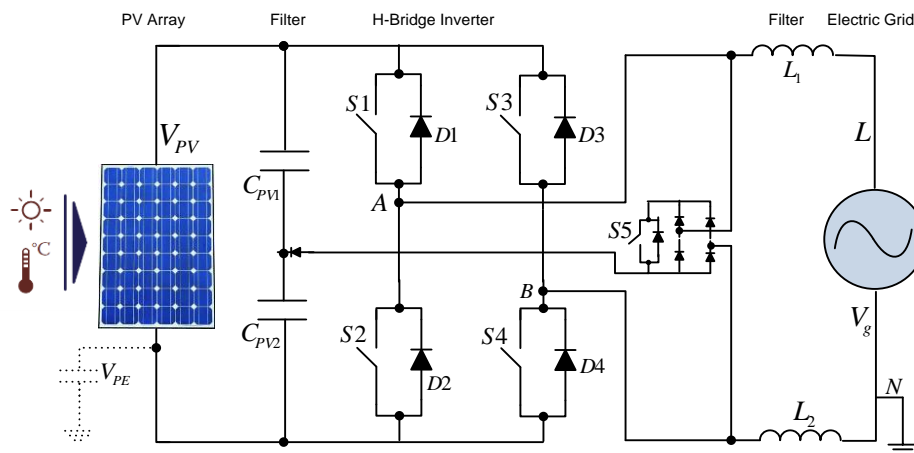


Figure 15. Schematic diagram of the FB-ZVR inverter [43,56].

Figure 16 presents the generation of AC currents for the positive and negative switching states. The main function of FB-ZVR topology is as follows:

- Like in bipolar modulation, the switches are diagonally switched in FB. The zero state is introduced by turning off all switches of the bridge except S_5 .

I. Advantages

For FB-ZVR, the following points were noted: (a) the core losses are lower due to unipolar voltage variation i.e., ($0 \rightarrow +V_{PV} \rightarrow 0 \rightarrow -V_{PV} \rightarrow 0$); (b) because of a lower switching frequency in one leg, and no exchange of reactive power between C_{PV} and $L_{1(2)}$ during zero voltage, its efficiency is higher, up to 96%; (c) The EMI filtering requirement and the leakage current peaks is lower as V_{PE} has no switching frequency component and only grid frequency component is present [56].

II. Disadvantages

Its disadvantages are: (a) addition of four extra diodes and one more switch; (b) filter losses increases, as bipolar output is obtained during deadtime clamping.

III. Analysis

In terms of low leakage and high efficiency, the advantageous of the HERIC are inherited by the FB-ZVR. The efficiency is lower than HERIC, because of the high switching frequency of S_5 , however, it has the advantage that it can work at any power factor [56].

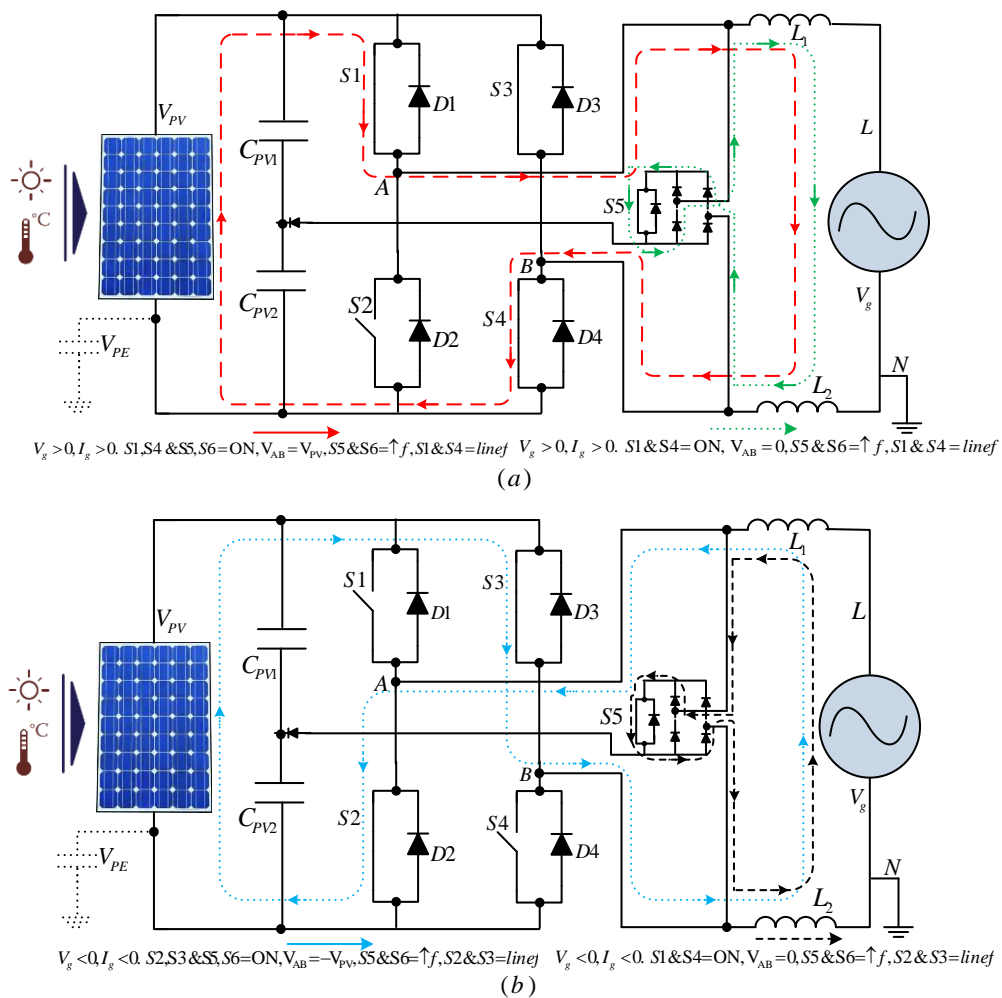


Figure 16. Switching positions of FB-ZVR in case of (a) positive cycle and (b) negative cycle [43,56].

3.7. FB-Derived Inverter Topologies: An Overview

Actually, the 2-level FB (or HB) converter can be modified into three level converters by using FB-DCBP, REFU, H5, and HERIC topologies. The input voltage stress on both output inductor and the switches are reduced to half thus increasing the efficiency. By using additional DC bypass (FB-DCBP) or AC bypass (REFU or HERIC) or higher switches of the bridge (H5), the zero-voltage condition is accomplished by shorting the grid. FB-DCBP and REFU clamp the neutral to the center point of the DC link while HERIC and H5 isolate the grid from the PV panels at zero voltage. Together HERIC and REFU use the AC bypass however, HERIC utilizes two switches in series (back to back) and REFU uses two switches in antiparallel configuration. Therefore, in the AC bypass for the REFU topology, the conduction losses are lower. The efficiency of H5 and REFU is to some extent higher in comparison to FB-DCBP and HERIC. H5 and REFU has only one switch that operate on high switching frequency while two switches are operated with high frequency in case of FB-DCBP and HERIC converters [43,46,56].

The implementation of the FB-ZVR is different, although it's derived from HERIC, it uses one switch and diode bridge as a bidirectional switch. This topology can also work with non-unitary power factor and have constant V_{PE} , but moderately high efficiency (higher than FB-BP but lower than HERIC).

4. NPC Based Inverter Structures

NPC was first introduced by Takahashi et al. in 1981 [66]. In comparison to the two-level FB inverter, NPC has lower switching stress as well as dV/dt . Because of the versatile nature of the NPC topology, it is effective in both three phase and single phase (HB or FB) systems. The NPC topology is the single-phase inverter operating with multi-level topology applied in high power motor operation.

4.1. NPC Half Bridge Inverter

The NPC HF inverter is based on the concept in which zero voltage is acquired by using D+ or D- based on the symbol of the current the output is clamped to central point (ground) of the DC bus, as presented in Figure 17 [67–70]. Figure 18 presents the generation of AC currents for the positive and negative switching states.

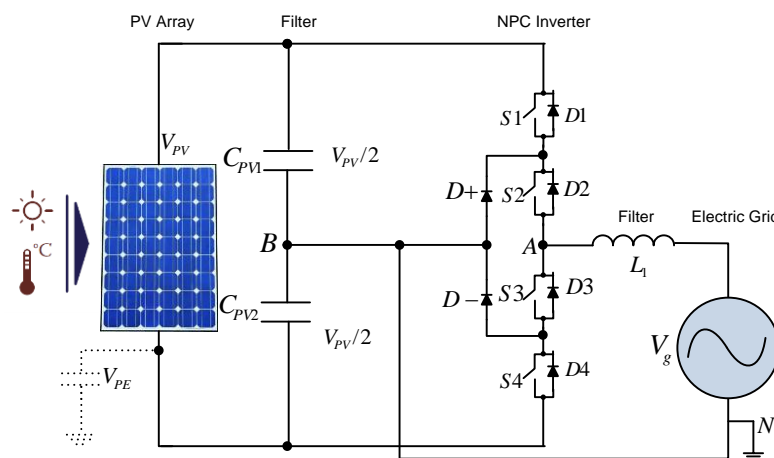


Figure 17. Schematic diagram of the FB-ZVR inverter [43,56].

The main functions of NPC HF topology are: (a) when boost is not needed: $V_{PV} > |V_g|$, The possible zero voltage conditions are: $S_3, D^- = \text{ON}$ and $S_2, D^+ = \text{ON}$ are switched at high frequency. In out of unitary power factors operation in resistance for $V_g > 0$ S_1 and S_3 , and for $V_g < 0$, $I_g > 0$ switches S_2 and S_4 are operated; (b) S_2 (S_3) are operating at grid frequency while the switching frequency of S_1 and S_4 are high [30].

I. Advantages

The FB-ZVR has the advantageous features: (a) the core losses are lower due to unipolar voltage variation i.e., $(0 \rightarrow +V_{PV} \rightarrow 0 \rightarrow -V_{PV} \rightarrow 0)$; (b) because there is no exchange of reactive power between C_{PV} and $L_{1(2)}$ during zero voltage and in one leg lower frequency switching, its efficiency is higher, up to 98%; (c) the EMI filtering requirement and the leakage current peaks is lower as V_{PE} is constant and is equal to $V_{PV}/4$ has no switching frequency component and only grid frequency component is present; (d) the reduction in the switching losses is because the outer switches voltage rating can be reduced to $V_{PV}/4$ [67,68].

II. Disadvantages

This topology has the following disadvantages: (a) addition of two more diodes; (b) in comparison with FB, double voltage input is needed; (c) the switching losses are unbalanced, lower on the middle switches and higher on the higher/lower switches; (d) in the neutral point addition of any inductance will lead to leakage current as EMI filters produces high-frequency common-mode voltage.

III. Analysis

In comparison with REFU, HERIC, and H5, The NPC HB is very similar in performance. Due to high efficiency, low filtering requirements, and low EMI, for use in transformerless PV system this topology is very appropriate. Currently, in the series called TripleLynx (three-phase 10/12.5/15 kW), it is marketed by Danfoss Solar Inverter, having 98% efficiency (Photon Magazine, July 2010) and a European efficiency of 97% [30,68].

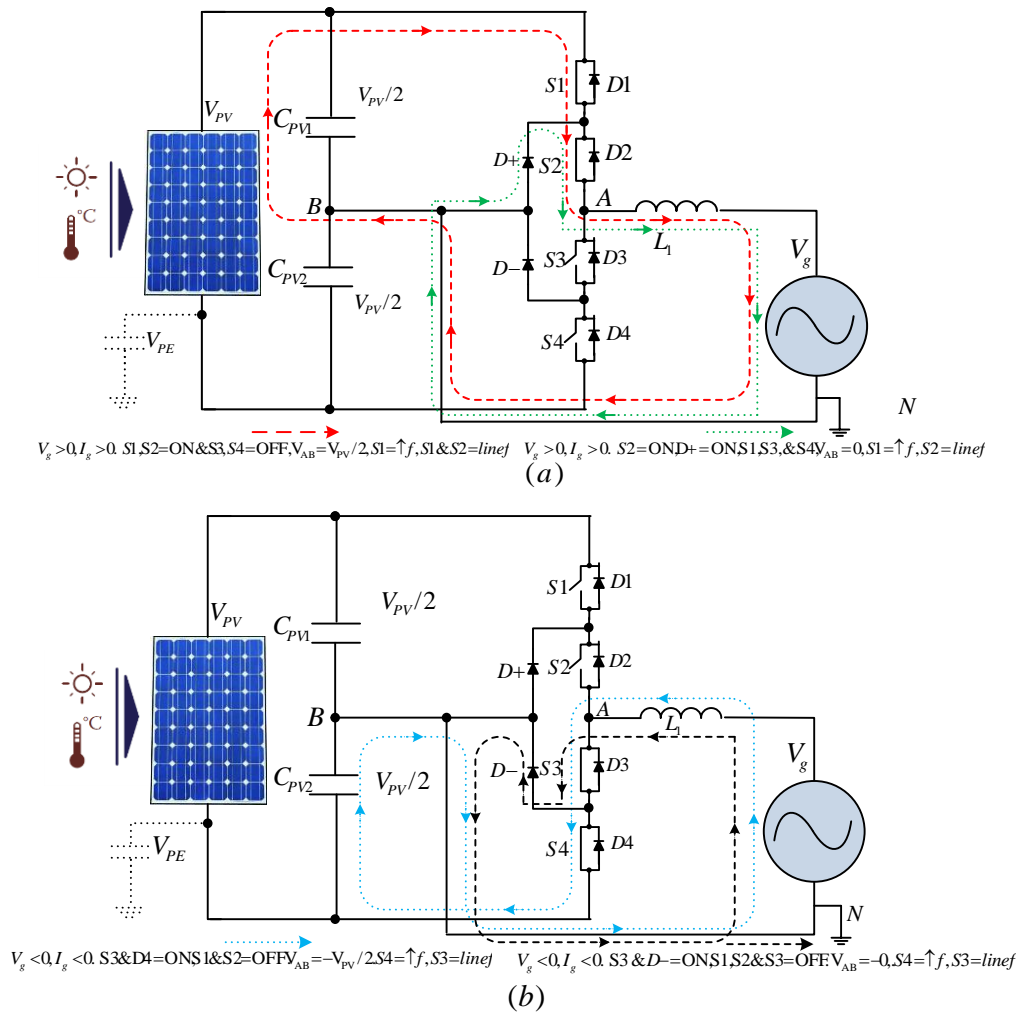


Figure 18. Switching positions of NPC HB in case of: (a) positive cycle and (b) negative cycle [29,30].

4.2. Conergy NPC Inverter

The variation of classical NPC yields to the HF topology whose output is clamped to the neutral using two back-to-back IGBTs based bidirectional switch. This topology is presented in Figure 19 and patent by Conergy [71]. An alternative of the same concept topology is depicted in [50], where instead of HB, a FB is used and in place of series connection, a parallel connection of unidirectional clamping switches is carried out.

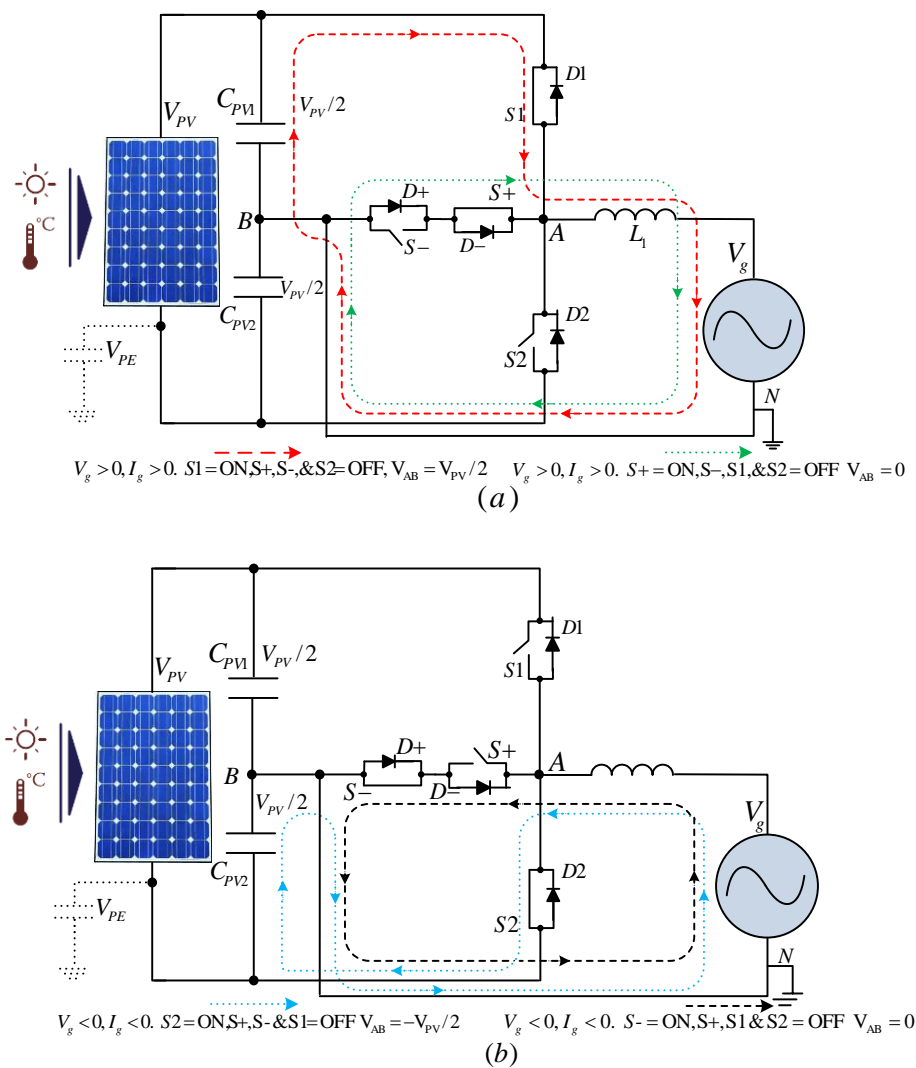


Figure 20. Switching positions of Conergy NPC in case of (a) positive cycle and (b) negative cycle [29,30].

4.3. Miscellaneous Topologies

Solar PV inverters with the grid-connected feature are characterized with mathematical models, and their utility in experimental tests and simulations with computer software are presented by Rampinelli et al [75]. A micro-inverter with grid-connected, phase-shift power modulation scheme, lesser passive components and with a decreased number of power conversion is suggested in [76]. In [77] an H-bridge multilevel inverter topology is suggested, with enhanced conversion efficiency from DC to AC storage of battery power to operate 24/7. A grid-connected nine level inverter topology using a low potential PV module to produce high voltage AC has been suggested in [78]. For the implementation of active power filter having the capability of power injection and static var compensator (SVC). The authors of [79] suggested an inverter topology having 27 levels. Barbosa et al. in [80] suggested a multilevel boost current inverter for grid-connected single-phase solar PV systems. In [81,82] different inverter topologies such as MOSFET inverter topology with H6-type technique, enhanced H6 topology, HB having a capacitor divider feature, HB designed with control circuit generation, H5 with optimized technology (oH5), grid connected multilevel inverter topology, high reliable and efficient (HRE) inverter topology, hybrid zero voltage rectifier topology (HR-ZVR), grid connected multifunction inverter topology, virtual DC bus topology, buck-boost converter, buck

converter, boost converter, and related topologies for solar PV grid-connected applications were addressed. Comparison of numerous transformerless single-phase inverter topologies have been presented in [76–82], which are applied in grid-connected PV solar systems.

4.4. NPC-Derived Inverter Topologies: An Overview

All the NPC-derived inverter topologies are three-level topologies. The advantageous features of these topologies are: (a) because of grounded DC link center practically no leakage current; (b) during the zero-voltage state, its efficiency is higher due to clamping of PV panels, and (c) unipolar voltage across the filter. In comparison with FB-derived topologies because of the higher complexity, with ratings over 10 kW (mini-central) three-phase inverters these topologies are typically used. Besides, in the range of hundreds of kW, i.e., high power (central inverter), where multilevel inverters are too significant, these topologies are also very attractive [43,76–82].

5. Transformerless PV Inverters: Comparative and Characteristics Overview

5.1. Parameter Comparison

The various topologies discussed, described, and analyzed till now are comprehensively compared in this section on the basis of different performance parameters such as number of input capacitors and capacitance, power semiconductors, output voltage, number of MPPTs, and leakage current as presented in Tables 1 and 2 [83].

Table 1. Comparative assessment of SPGC transformerless inverter topologies [43].

IT/PI	HBT	FBT	HT	H5 T	H6 T	NPC T	A-NPC T	FCT	C-NPC T
IC	2	1	1	1	2	2	2	3	2
S	2	4	6	5	6	4	6	4	4
D	0	0	2	0	2	2	0	0	0
OVL	2	3	3	3	3	3	3	3	3
NM	1	1	1	1	1	1	1	1	1
LC	VL	H	VL	VL	VL	VL	VL	VL	VL
ME	-	-	-	98.5	97.4	98.16	97.34	-	97.67
TV	800	400	400	400	600	400	400	400	400
IC	H	L	L	L	H	H	H	H	H
C	L	M	H	H	H	M	H	M	M

Note: IT/PI: Inverter Types/Performance Indices, HBT: Half Bridge Topology, FBT: Full Bridge Topology, HT: HERIC Topology, H5 T: H5 Topology, H6 T: H6 Topology, NPC T: NPC Topology, A-NPC T: Active NPC Topology, FCT: Flying Capacitor Topology, C-NPC T: Conergy-NPC Topology, IC: Input Capacitor, S: Switches, D: Diode, OVL: Output Voltage Level, LC: Leakage Current, NM: Number of MPPT, VL: Very Low, H: High, ME: Maximum Efficiency (%), TV: Transistor Voltage (V), IC: Input Capacitance, L: Low, C: Cost, M: Medium

The cost of the converter directly affects the number of switches, that's why a minimum number of power switches are preferable. A good output current is obtainable from a good output voltage, which is easy to filter out. To regulate the power acquired from the PV modules, the control of input voltage is important which is carried out by number of MPPTs. Leakage current reduction in the transformerless inverters is mandatory.

Table 2. Comparison of various transformerless inverter topologies [48,63,66,68,84–94].

R	T	IV (V)	LC	S	E (%)	D	A
[87]	HB	700	M	2 T	*	Voltage stress in DC-link is high	Cost is low
[88]	C-NPC	800	VL	3 T+ 4 D	**	Device stress is high	Conduction losses is low
[89]	FB	400	M	4 T	*	Leakage current is high	-
[90]	NPC	400	VL	4 T + 2 D	**	Device stress is high	Leakage current is very low
[91]	D-B	400	L	4 T + 2 D	****	Extra devices required	Efficiency is high
[92]	T-LNPC	800	VL	4 T + 2 D	***	Complexity is high	Leakage current is very low
[93]	H5	400	L	5 T	***	Switching unbalance	Component count is low
[94]	S-B	400	M	5 T + 1 D	**	Leakage current is high	Filter inductor is only one
[95]	VDCB	400	L	5 T	**	Switch 5 current stress	Filter inductor is only one
[96]	HB-ZVR	400	L	5 T + 5 D	*	Complexity is high efficiency is low	-
[97]	H	400	L	6 T + 2 D	***	Extra devices required	Line frequency leakage current
[98]	H6	400	L	6 T + 2 D	**	Extra devices required	Line frequency leakage current
[99]	HRE	400	L	6 T + 6 D	****	Complexity is high	Efficiency is very high
[100]	oH5	400	VL	6 T	***	Extra devices required	Leakage current is very low
[101]	C	400	M	8 T	-	Extra devices required and complex control	Lower THD & commutation

Note: R: Reference, T: Topologies, IV: Input Voltage, LC: Leakage Current, S: Switches, E: Efficiency, A: Advantages, HB: Half Bridge, C-NPC: Conergy NPC, FB: Full Bridge, D-B: Dual-Buck, T-LNPC: Three-Level NPC, S-B: Single-Buck, VDCB: Virtual DC Bus, H: HERIC, C: Cascaded, VL: Very Low, M: Moderate, T: Transistor, D: Diode, D: Disadvantageous, A: Advantageous, *: very low, **: low, ***: high, ****: very high.

5.2. Loss Analysis

Using the thermal module in PSIM, loss analysis is carried out. The specifications of the system and parameters of devices are listed in Table 3. Switching losses and conduction losses are the two main losses occurs in PV systems. Equations (1) and (2) calculate the switching losses and conduction losses for IGBT and diode, respectively:

$$\left. \begin{aligned} P_{SW-ON} &= E_{ON} \times f \times V_{cc} / V_{cc\text{datasheet}} \\ P_{SW-OFF} &= E_{OFF} \times f \times V_{cc} / V_{cc\text{datasheet}} \\ P_{SW-IGBT} &= P_{SW-ON} + P_{SW-OFF} \\ P_{SW-Diode} &= P_{ON-Diode} + P_{OFF-Diode} \end{aligned} \right\} \quad (1)$$

where is P_{SW-ON} turn on losses and turn off losses P_{SW-OFF} , E_{ON} are turn on and E_{OFF} turn of energy losses:

$$\left. \begin{aligned} P_{Con-IGBT} &= V_{CE(SAT)} \times I_F \\ P_{Con-Diode} &= V_F \times I_F \end{aligned} \right\} \quad (2)$$

Table 3. Specification for loss calculation.

Parameters for Losses Simulation		Parameters for Universal Simulation	
Parameter	Value	Parameter	Value
Device	GT50J325	Input voltage	400 V _{dc}
Frequency	50 Hz	Load	100 ohm
Saturation voltage Vce (SAT)	2 V	Rated power	1 kW
Forward Voltage, VF	2.5 V	Switching Frequency	10 kHz
Junction temperature, Tj (max)	150 °C	Dead Time	2.5 us
Turn-on energy losses, Eon@Vdc = 300V	1.30 mJ	DC-link capacitors	2200 uF, Vdc = 400 V
Turn-off energy losses, Eoff@dc = 300V	1.34 mJ	IGBT	GT50J325 V _{CE} = 600 V, I _C = 60 A
Pcond_Q calibration factor	1	Fast-recovery diodes	RHRP30120 V _{RR} = 1200 V, I = 30 A
Psw_Q calibration factor	1	Filter inductors	3 mH
Pcond_D calibration factor	1	Filter capacitors	6 nF
Psw_D calibration factor	1	Stray capacitors	100 nF

The AC-decoupling topologies i.e., HERIC, HBZVR, and HBZVR-D have lower losses in comparison to the DC-decoupling topologies i.e., H5, oH5, and H6. Because of the large components

in its conduction path the H6 topology has the highest device losses. HERIC has slightly lower losses than HBZVR, and HBZVR-D. Since VDC is the same, the influence of DC-link voltage is small in all topologies. Because of three level unipolar output voltage the influence of ripple currents of filter inductor is negligible. Additionally, switching losses and total losses are also mentioned in Figure 21.

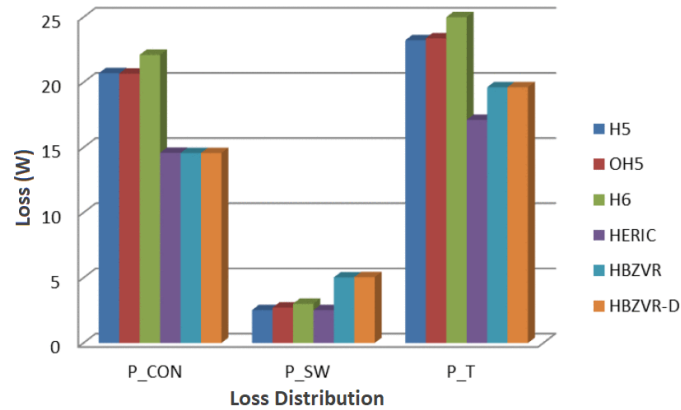


Figure 21. Loss distribution of various topologies at 1 kW.

6. Control Structure for Single Phase and Three Phase Grid Connected Systems

Transformerless PV based inverter structures are elaborated in this survey. Conversely, the final structure will be different as most of them require boosting. Subsequently, the power of a single PV panel is low and strongly reliant on ambient temperature and solar irradiance (ambient conditions), therefore either a buck-boost or boost converter is required to attain an adequate DC-link voltage [95–99].

Figure 22 presents a H-bridge boosting PV inverter with low-frequency transformer, with high-frequency transformer, and without transformer, respectively. Additionally, high-frequency versions (HERIC or H5) can easily replace the FB inverter.

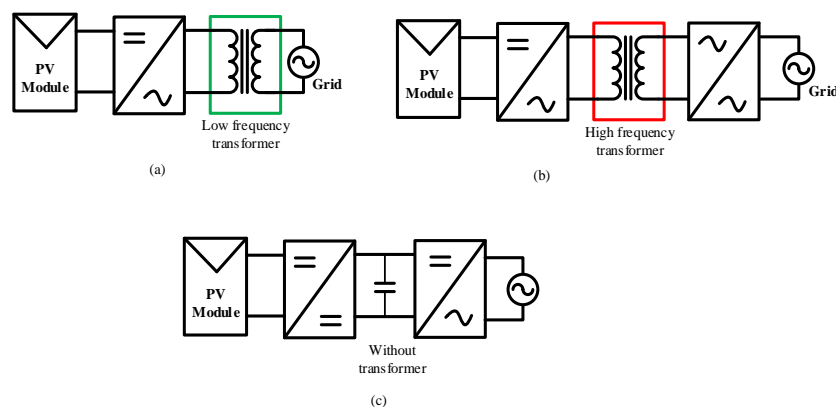


Figure 22. H-Bridge based PV inverter with: (a) low-frequency transformer, (b) high-frequency transformer, (c) without a transformer [30] Control is important in order to utilize and transfer to grid the generated power effectively. The following section details the generic, single phase, and three phase control structures of grid connected PV system.

6.1. Generic Control Structure

The main purpose of the control for single phase grid-connected systems (SPG-CS) are: (a) to maximize the power from PV panels, the PV-side control is incorporated; (b) for the purpose of fulfilling the demands to the power grid, the grid-side control is performed. In order to satisfy the

requirements/demands, the generic control structure comprises of two cascaded loops [100,101]. The inner control loop is accountable for shaping the current while outer voltage/power control loop produces the current command. In this way, the quality of power is sustained along with various other functionalities as depicted in Figure 23. The two-main classifications of the control are:

- MPP control: MPP control is used to extract maximum power from solar PV modules.
- Inverter control: This control is used to (a) inject quality power and stay synchronize with the grid, (b) control the power flow to the grid and (c) maintain DC link voltage at desired level.

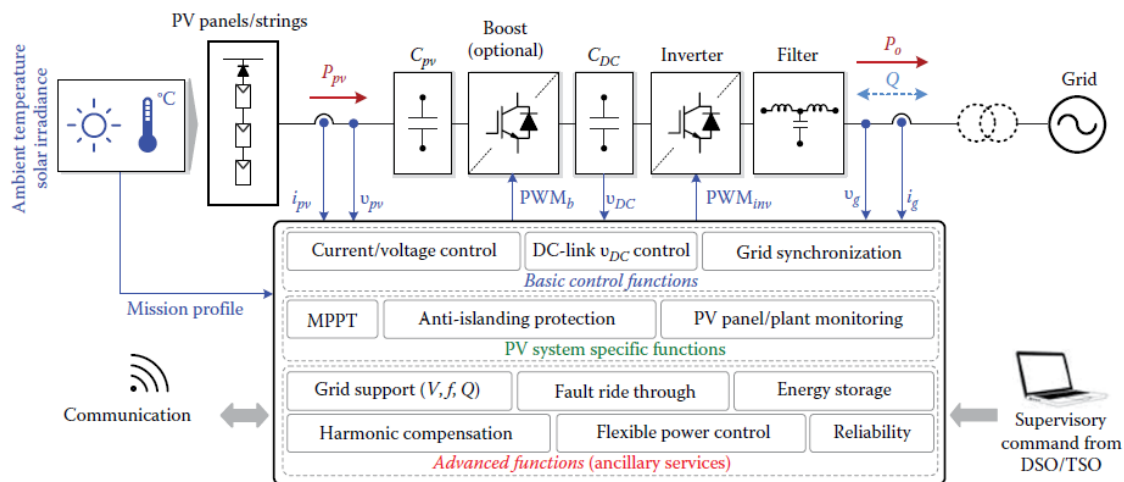


Figure 23. Generic control structure for Single phase grid-connected system [29,101].

The distributed system connected to the grid is of main importance, the disturbances when no suitable controllers are designed and grid instability are the problems associated with grid-connected distributed system. According to their applications, the controllers are separated into six categories i.e., Predictive controllers, robust controllers, linear and non-linear controllers, intelligent controllers and adaptive controllers [29,43].

6.2. Single phase and Three Phase Control Structure

The control structure of PV inverters is composed of two cascaded loops. The response of the inner loop is faster than that of the outer loop. The inner loop is used to control grid currents that in turn regulate the injected active and reactive power to the grid, while the outer loop is a slow voltage regulating loop, that is used to control the DC link voltage of the inverter. The performance of these loops has a direct effect on the quality of output power and current protection. The significant characteristics of inner current loop controllers include faster response and harmonic compensation in the case of distorted grids, while the characteristics of outer loop controllers is to balance the power flow between the the grid and the PV system. Generally, the main fractures of the outer controller include optimal regulation and stabilized slow dynamical response of the system. The inner current control loop is (approximately) 5 to 20 times faster than the outer voltage control loop at achieving stability of the system. As the grid current and DC link voltage are separately controlled, hence the transfer function of the inner loop is not required in the design procedure of outer loop controllers, i.e., a DC link voltage controller [101,102]. However, some researchers have also proposed a cascaded voltage control loop and power control loop. As an alternative to the current control loop, the power control loop will indirectly control the current injected into the grid. Table 4 shows the detailed characteristics of control structures for single phase PV inverters, while Table 5 summarize the feature of three phase inverter control. The d and q component shown in Table 5 are used to control active power plus DC link voltage and reactive power, respectively.

Table 4. Control configurations for single-phase inverters [103].

Topologies	Advantage	Disadvantages	Figures
DC/DC converter based Single phase inverter	<ul style="list-style-type: none"> ○ Current control is instantaneous ○ Dynamic response is fast 	<ul style="list-style-type: none"> ○ Power factor control is not full ○ Hardware circuit is complex 	Figure 24a
Single phase inverter without DC/DC converter	<ul style="list-style-type: none"> ○ Conversion system is simplicity ○ Current control is instantaneous ○ Dynamic response is fast 	<ul style="list-style-type: none"> ○ Hardware circuit is complex ○ Power factor control is not full 	Figure 24b
Single phase inverter with PCSP	<ul style="list-style-type: none"> ○ Control of reactive power ○ Simple circuitry ○ Simplicity ○ Few resources 	<ul style="list-style-type: none"> ○ Insufficient current control ○ Slow dynamics 	Figure 24c

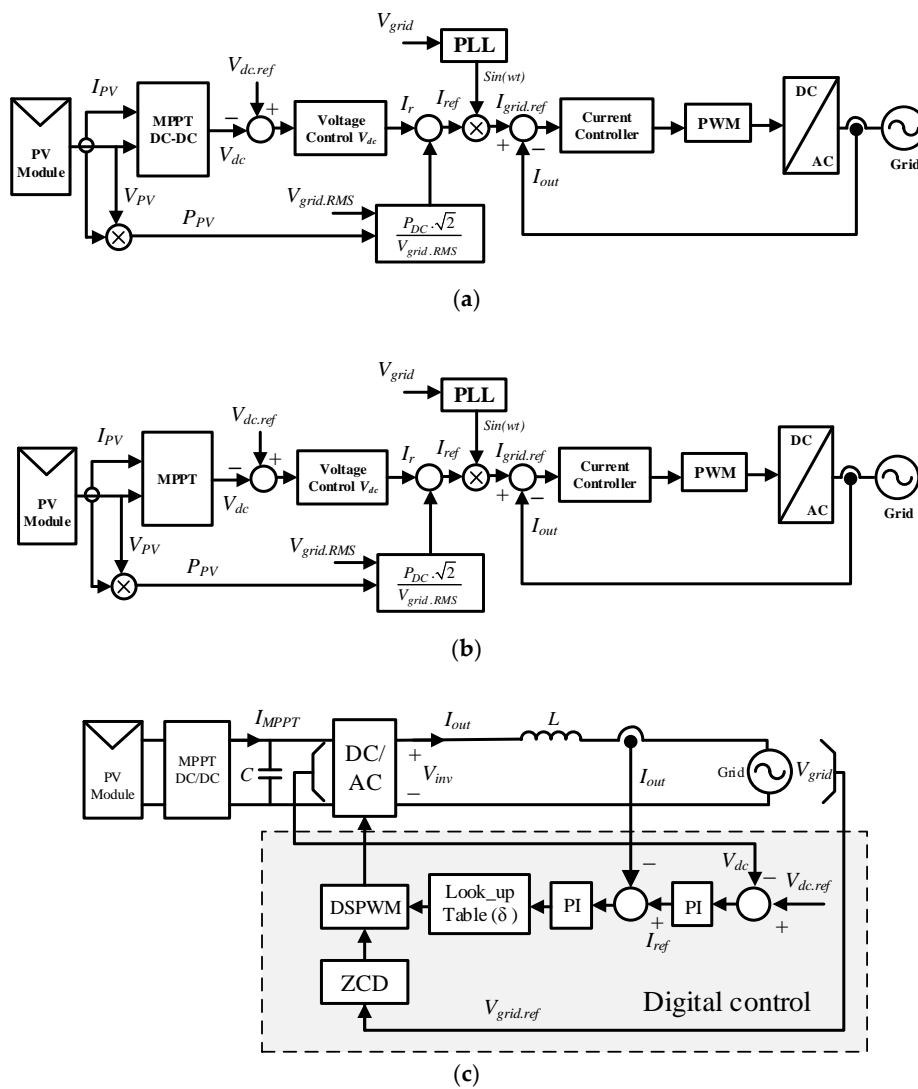


Figure 24. Configurations for single-phase inverters (a) DC/DC converter based single phase inverter; (b) Single phase inverter without DC/DC converter; (c) Single phase inverter with PCSP.

Table 5. Control structures for three-phase inverters [55,104].

Topologies	Control Equations	Advantage	Inconvenient	Figures	Controller Type
dq control	$P = 3/2(e_d i_d + e_q i_q)$ or $P = 3/2e_d i_d$ when $e_q = 0$; $Q = 3/2(e_q i_d - e_d i_q)$ or $Q = -3/2e_d i_q$ when $e_q = 0$	<ul style="list-style-type: none"> ○ Simplicity ○ Controlling and filtering can be easier accomplished 	<ul style="list-style-type: none"> ○ The steady-state error is not removed ○ Compensation capability of the low-order harmonics is very poor 	Figure 25a	PI
$\alpha\beta$-control	$P = 3/2(e_\alpha i_\alpha + e_\beta i_\beta)$ or $P = 3/2e_\alpha i_\alpha$ when $e_\beta = 0$; $Q = 3/2(e_\beta i_\alpha - e_\alpha i_\beta)$ or $Q = -3/2e_\alpha i_\beta$ when $e_\beta = 0$	<ul style="list-style-type: none"> ○ The steady-state error is removed ○ Around the resonance frequency, a very high gain is acquired ○ High dynamic 	<ul style="list-style-type: none"> ○ Complex Hardware circuit ○ No complete control of power factor 	Figure 25b	PR
abc control	$G_{PR}^{(abc)}(s) = \begin{bmatrix} K_p + \frac{K_i s}{s^2 + \omega_0^2} & 0 & 0 \\ 0 & K_p + \frac{K_i s}{s^2 + \omega_0^2} & 0 \\ 0 & 0 & K_p + \frac{K_i s}{s^2 + \omega_0^2} \end{bmatrix}$ $v_{dq0} = [T_\theta] v_{abc}$	<ul style="list-style-type: none"> ○ Simple transfer function ○ High dynamic ○ Rapid development ○ High dynamic. ○ Simple control for current regulation. ○ Rapid development 	<ul style="list-style-type: none"> ○ The transfer function is complex ○ More complex than hysteresis and Deadbeat ○ High complexity of the control for current regulation. ○ Implementation in high frequency microcontroller 	Figure 25c	PI PR Hysteresis Dead-Beat

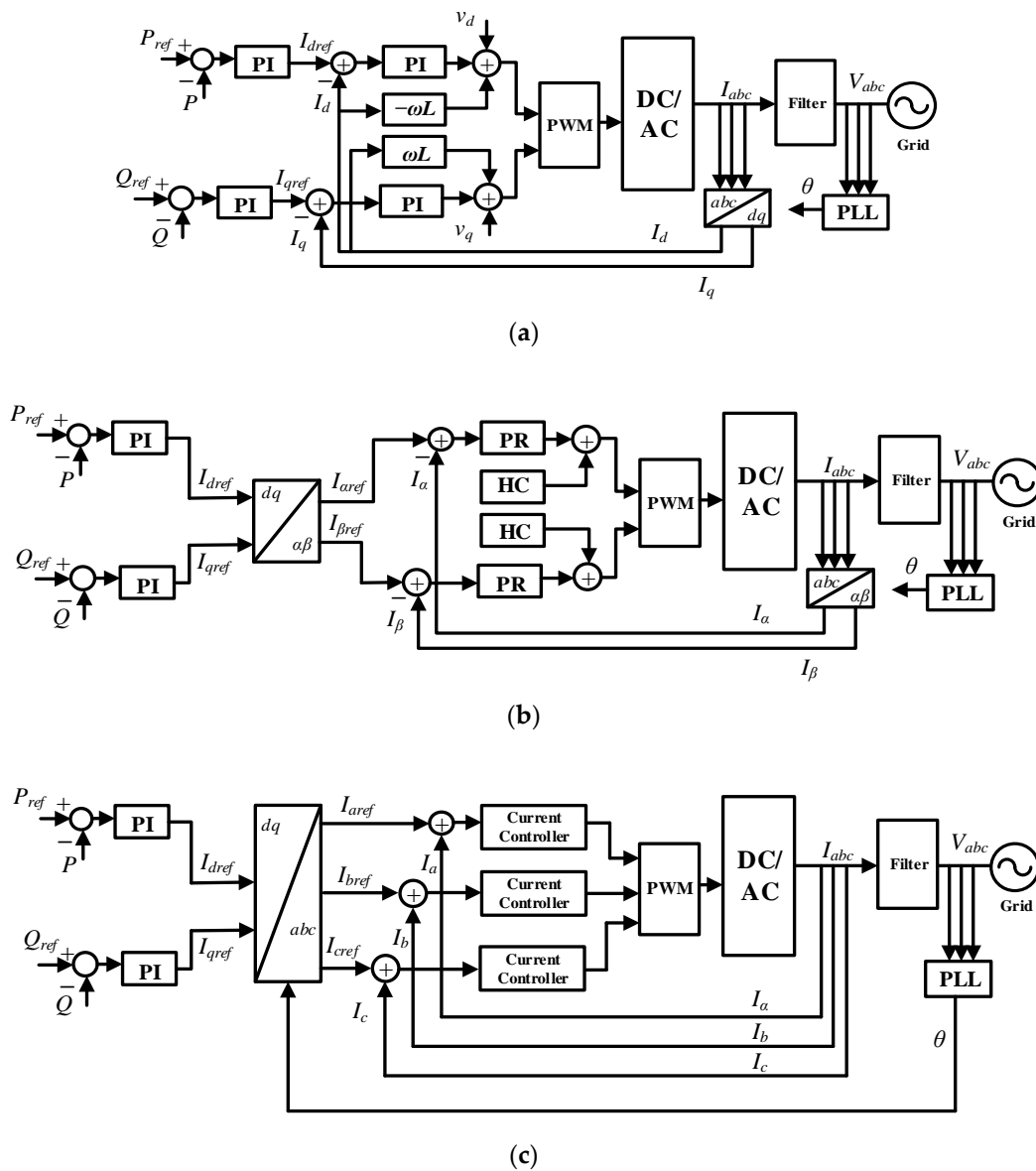


Figure 25. Control structures for three-phase inverters. (a) dq control; (b) $\alpha\beta$ -control; (c) abc control.

7. Conclusions and Future Work

Grid-tied inverters are the vital components for the effective interface of RER and utility in the distributed generation system. Currently, single-phase transformerless grid-connected photovoltaic (SPTG-CPV) inverters (1–10 kW) are attracting additional consideration. In comparison to the transformer (TR) GI-based inverters, their advantageous features are lower cost, lighter weight, smaller volume, higher efficiency, and less complexity. Based on leakage current minimization approaches these topologies are principally categorized as: GI with CMV clamping and without CMV clamping. By incorporating extra switches, the GI can be acquired either on DC side or the AC side of H-Bridge or NPC topology.

The technological development in power electronics sector have brought high efficiency and large varieties of transformerless inverters into existence that are derived from the H-bridge inverter. These derived inverter topologies have higher efficiencies and low EMI/CM. In this paper, a survey of grid-connected single-phase photovoltaic inverters based on transformerless topologies has been presented. The basic operational principle of all SPTG-CPV inverters is presented for positive, negative,

and zero cycles in details. The advantages, disadvantages, and a complete analysis of each topology are also reviewed in this survey. A comparative assessment is also performed based on weaknesses, strengths, component ratings, efficiency, total harmonic distortion (THD), semiconductor device losses, and leakage current of various SPTG-CPV inverter schemes. Loss analysis for various grid connected transformerless inverter topologies at 1 kW is presented. Control schemes for grid connected three-phase system and single-phase PV systems are also discussed, described and reviewed in detail.

The conclusion of the review is that the efficiency of AC side decoupled topologies (HERIC, REFU, FBZVR) is high in comparison with DC side decoupled topologies (H5, FB-DCBP). This is due to the independency and isolation of AC bypass switches from the conduction path. This significantly reduces the conduction losses by providing a freewheeling path. In addition, in terms of loss, the AC-decoupling device family is superior to the DC-decoupling family. Losses analysis and study are useful for the engineer to choose and design the high-efficiency transformerless topology. In comparison with FB-derived topologies because of the higher complexity, with ratings over 10 kW (mini-central) three-phase inverters NPC topologies are typically used. Besides, in the range of hundreds of kW, i.e., high power (central inverter), where multilevel inverters are too significant, NPC topologies are also very attractive.

In the near future, the understanding of power converters is necessary for integration of RER (i.e., solar PV) with the grid and fulfilling the grid code requirements provided by the grid operator with a minimum harmonic injection. Currently, low-efficiency PV arrays are available, to ensure maximum efficiency investigation into the materials for the fabrication of the PV panels is also needed. Additionally, the overall performance and efficiency of grid-connected solar PV system will improve, and costs will be minimized. The new topologies of grid connected inverters are in a progressive stage since last decade. The main focus area of this research is increasing the power density and reliability, improving the efficiency of overall performance of power converters. There are also certain important topics in transformerless inverter that are: (a) utilization of multilevel transformerless inverters to achieve medium voltage for grid connection; (b) future power conditioner Quasi Z Source Network (c) development of power storage converters having LVRT capability. Furthermore, in the near future SiC will mostly use as a power device in converters and modification of GaN converters with SiC devices will usher in a new era of power converters by enhancing the efficiency of converters. In addition, the emergence of thin-film PV panels and wide-bandgap devices will probably steer the research in new directions, modifying the landscape of the most effective and most widespread converter architectures. The authors expect that this survey will prove as a benchmark for researchers, creators, engineers and designers working in the field of transformerless PV inverters. Furthermore, it will help users select relevant topologies for their specific applications.

Author Contributions: K.Z., and W.U. propose the main idea of the paper. The paper is written by K.Z. and I.K. and is revised by M.A.K., P.S., T.D., C.B., Iftikhar Ahmad. All the authors were involved in preparing the final version of this manuscript. Besides, this whole work is supervised by H.J.K.

Acknowledgments: This research was supported by Basic Research Laboratory through the National Research Foundations of Korea funded by the Ministry of Science, ICT and Future Planning (NRF-2015R1A4A1041584).

Conflicts of Interest: The authors declare no conflict of interest.

References

1. Hassaine, L.; Olias, E.; Quintero, J.; Salas, V. Overview of power inverter topologies and control structures for grid connected photovoltaic systems. *Renew. Sustain. Energy Rev.* **2014**, *30*, 796–807. [[CrossRef](#)]
2. Ellabban, O.; Abu-Rub, H.; Blaabjerg, F. Renewable energy resources: Current status, future prospects and their enabling technology. *Renew. Sustain. Energy Rev.* **2014**, *39*, 748–764. [[CrossRef](#)]
3. Zeb, K.; Uddin, W.; Khan, M.A.; Ali, Z.; Ali, M.U.; Christofides, N.; Kim, H.J. A comprehensive review on inverter topologies and control strategies for grid connected photovoltaic system. *Renew. Sustain. Energy Rev.* **2018**, *94*, 1120–1141. [[CrossRef](#)]

4. Sawin, J.L.; Seyboth, K.; Sverrisson, F. *Renewables 2016: Global Status Report*; REN21: Ottawa, ON, Canada, 2016.
5. Wirth, H. *Recent Facts about Photovoltaics in Germany*; Fraunhofer Institute for Solar Energy Systems ISE: Fraunhofer, Germany, 2015.
6. SolarPower Europe. Global Market Outlook for Solar Power 2015–2019. 2014. Available online: https://helapco.gr/pdf/Global_Market_Outlook_2015_-2019_lr_v23.pdf (accessed on 24 July 2018).
7. Wind Energy and Solar | Installed GW Capacity-Global and by Country. Available online: <http://www.fipowerweb.com/Renewable-Energy.html> (accessed on 20 July 2018).
8. Blaabjerg, F.; Ma, K.; Yang, Y. Power electronics-The key technology for renewable energy systems integration. In Proceedings of the 2015 International Conference on Renewable Energy Research and Applications (ICRERA), Palermo, Italy, 22–25 November 2015.
9. Van Wyk, J.D.; Lee, F.C. On a Future for Power Electronics. *Emerg. Sel. Top. Power Electron. IEEE J.* **2013**, *1*, 59–72. [[CrossRef](#)]
10. Kjaer, S.B.; Pedersen, J.K.; Blaabjerg, F. A review of single-phase grid-connected inverters for photovoltaic modules. *IEEE Trans. Ind. Appl.* **2005**, *41*, 1292–1306. [[CrossRef](#)]
11. Bergveld, H.J.; Büthker, D.; Castello, C.; Doorn, T.; de Jong, A.; van Otten, R.; de Waal, K. Module-Level DC/DC Conversion for Photovoltaic Systems: The Delta-Conversion Concept. *IEEE Trans. Power Electron.* **2013**, *28*, 2005–2013. [[CrossRef](#)]
12. Liu, B.; Duan, S.; Cai, T. Photovoltaic DC-Building-Module-Based BIPV System-Concept and Design Considerations. *Power Electron. IEEE Trans.* **2011**, *26*, 1418–1429. [[CrossRef](#)]
13. Sera, D.; Mathe, L.; Blaabjerg, F. Distributed control of PV strings with Module Integrated Converters in presence of a central MPPT. In Proceedings of the 2014 IEEE Energy Conversion Congress and Exposition (ECCE), Pittsburgh, PA, USA, 14–18 September 2014.
14. Eltawil, M.A.; Zhao, Z. Grid-connected photovoltaic power systems: Technical and potential problems-A review. *Renew. Sustain. Energy Rev.* **2010**, *14*, 112–129. [[CrossRef](#)]
15. Spertino, F.; Graditi, G. Power conditioning units in grid-connected photovoltaic systems: A comparison with different technologies and wide range of power ratings. *Sol. Energy* **2014**, *108*, 219–229. [[CrossRef](#)]
16. Zeb, K.; Ali, Z.; Saleem, K.; Uddin, W.; Javed, M.A.; Christofides, N. Indirect field-oriented control of induction motor drive based on adaptive fuzzy logic controller. *Electr. Eng.* **2017**, *99*, 803–815. [[CrossRef](#)]
17. Romero-Cadaval, E.; Spagnuolo, G.; Franquelo, L.G.; Ramos-Paja, C.A.; Suntio, T.; Xiao, W.M. Grid-connected photovoltaic generation plants: Components and operation. *IEEE Ind. Electron. Mag.* **2013**, *7*, 6–20. [[CrossRef](#)]
18. Meinhardt, M.; Cramer, G. Multi-String-Converter: The next step in Evolution of String-Converter Technology. In Proceedings of the 9th European Conference on Power Electronics and Applications, Graz, Austria, 15 March 2001.
19. Morjaria, M.; Anichkov, D.; Chadliev, V.; Soni, S. A Grid-Friendly Plant: The Role of Utility-Scale Photovoltaic Plants in Grid Stability and Reliability. *IEEE Power Energy Mag.* **2014**, *12*, 87–95. [[CrossRef](#)]
20. Zeb, K.; Ayesha; Haider, A.; Uddin, W.; Qureshi, M.B.; Mehmood, C.A.; Jazlan, A.; Sreeram, V. Indirect Vector Control of Induction Motor using Adaptive Sliding Mode Controller. In Proceedings of the 2016 Australian Control Conference (AuCC), Newcastle, NSW, Australia, 3–4 November 2016.
21. Li, Q.; Wolfs, P. A review of the single phase photovoltaic module integrated converter topologies with three different DC link configurations. *IEEE Trans. Power Electron.* **2008**, *23*, 1320–1333.
22. Yang, Y.; Enjeti, P.; Blaabjerg, F.; Wang, H. Wide-scale adoption of photovoltaic energy: Grid code modifications are explored in the distribution grid. *IEEE Ind. Appl. Mag.* **2015**, *21*, 21–31. [[CrossRef](#)]
23. He, J.; Yi, L.; Wang, X.; Wang, J. Research on deadbeat control of a three-level grid-connected inverter based on $\alpha\beta$ transform. *Procedia Eng.* **2011**, *23*, 397–402.
24. Kahrobaeian, A.; Farhangi, S. Stationary frame current control of single phase grid connected PV inverters. In Proceedings of the 2010 1st Power Electronic & Drive Systems & Technologies Conference (PEDSTC), Tehran, Iran, 17–18 February 2010.
25. Kaundinya, D.P.; Balachandra, P.; Ravindranath, N.H. Grid-connected versus stand-alone energy systems for decentralized power-A review of literature. *Renew. Sustain. Energy Rev.* **2009**, *13*, 2041–2050. [[CrossRef](#)]
26. Kazmierkowski, M.P.; Krishnan, R.; Blaabjerg, F.; Irwin, J.D. *Control in Power Electronics: Selected Problems*; Academic Press: Cambridge, MA, USA, 2002.

27. Kerekes, T.; Teodorescu, R.; Liserre, M.; Klumpner, C.; Sumner, M. Evaluation of three-phase transformerless photovoltaic inverter topologies. *IEEE Trans. Power Electron.* **2009**, *24*, 2202–2211. [[CrossRef](#)]
28. Özkan, Z.; Hava, A.M. Classification of grid connected transformerless PV inverters with a focus on the leakage current characteristics and extension of topology families. *J. Power Electron.* **2015**, *15*, 256–267. [[CrossRef](#)]
29. Blaabjerg, F.; Ionel, D.M. *Renewable Energy Devices and Systems with Simulations in MATLAB and ANSYS*; CRC Press: London, UK, 2017.
30. Teodorescu, R.; Liserre, M.; Rodríguez, P. *Grid Converters for Photovoltaic and Wind Power Systems*; John Wiley and Son, Ltd.: Chichester, UK, 2010.
31. Ahmad, Z.; Singh, S.N. Comparative analysis of single phase transformerless inverter topologies for grid connected PV system. *Sol. Energy* **2017**, *149*, 245–271. [[CrossRef](#)]
32. Yuan, X.; Merk, W.; Stemmler, H.; Allmeling, J. Stationary-frame generalized integrators for current control of active power filters with zero steady-state error for current harmonics of concern under unbalanced and distorted operating conditions. *IEEE Trans. Industry Appl.* **2002**, *38*, 523–532. [[CrossRef](#)]
33. Zhang, R.; Cardinal, M.; Szczesny, P.; Dame, M. A Grid Simulator with control of single-phase power converters in D-Q rotating frame. In Proceedings of the 2002 IEEE 33rd Annual IEEE Power Electronics Specialists Conference. Proceedings (Cat. No. 02CH37289), Cairns, Australia, 23–27 June 2002.
34. Zhu, H.; Arnet, B.; Haines, L.; Shaffer, E.; Lai, J.-S. Grid synchronization control without AC voltage sensors. In Proceedings of the Eighteenth Annual IEEE Applied Power Electronics Conference and Exposition, 2003 (APEC'03), Miami Beach, FL, USA, 9–13 February 2003.
35. Zmood, D.N.; Holmes, D.G. Stationary frame current regulation of PWM inverters with zero steady-state error. *IEEE Trans. Power Electron.* **2003**, *18*, 814–822. [[CrossRef](#)]
36. Hamrouni, N.; Jraidi, M.; Chérif, A. New control strategy for 2-stage grid-connected photovoltaic power system. *Renew. Energy* **2008**, *33*, 2212–2221. [[CrossRef](#)]
37. Yang, B.; Li, W.; Gu, Y.; Cui, W.; He, X. Improved transformerless inverter with common-mode leakage current elimination for a photovoltaic grid-connected power system. *IEEE Trans. Power Electron.* **2012**, *22*, 752–762. [[CrossRef](#)]
38. Hong, F.; Shan, R.Z.; Wang, H.Z. Analysis and calculation of inverter power loss. IEEE Std 1547.1-2005. IEEE Standards conformance Test Procedure for equipment interconnecting distributed resources with electric power system. *Pro. CSEE* **2008**, *28*, 72–78.
39. Mekhilef, S.; Islam, M. H6-type transformerless single-phase inverter for grid-tied photovoltaic system. *IET Power Electron.* **2015**, *8*, 636–644.
40. Islam, M.; Mekhilef, S.; Hasan, M. Single phase transformerless inverter topologies for grid-tied photovoltaic system: A review. *Renew. Sustain. Energy Rev.* **2015**, *45*, 69–86. [[CrossRef](#)]
41. Ji, B.; Wang, J.; Zhao, J. High-efficiency single-phase transformerless PV H6 inverter with hybrid modulation method. *IEEE Trans. Ind. Electron.* **2013**, *60*, 2104–2115. [[CrossRef](#)]
42. Chatterjee, S.; Kumar, P.; Chatterjee, S. A techno-commercial review on grid connected photovoltaic system. *Renew. Sustain. Energy Rev.* **2018**, *81*, 2371–2397. [[CrossRef](#)]
43. Patrao, I.; Figueres, E.; González-Espín, F.; Garcerá, G. Transformerless topologies for grid-connected single-phase photovoltaic inverters. *Renew. Sustain. Energy Rev.* **2011**, *15*, 3423–3431. [[CrossRef](#)]
44. Calais, M.; Agelidis, V.G.; Meinhardt, M. Multilevel converters for single-phase grid connected photovoltaic systems: An overview. *Sol. Energy* **1999**, *66*, 325–335. [[CrossRef](#)]
45. Xue, Y.; Manjrekar, M. A new class of single-phase multilevel inverters. In Proceedings of the 2nd International Symposium on Power Electronics for Distributed Generation Systems, Hefei, China, 16–18 June 2010.
46. Li, W.; Gu, Y.; Luo, H.; Cui, W.; He, X.; Xia, C. Topology review and derivation methodology of single-phase transformerless photovoltaic inverters for leakage current suppression. *IEEE Trans. Ind. Electron.* **2015**, *62*, 4537–4551. [[CrossRef](#)]
47. Boonmee, C.; Kumsuwan, Y. A phase-shifted carrier-based PWM technique for cascaded h-bridge inverters application in standalone PV system. In Proceedings of the 2012 15th International Power Electronics and Motion Control Conference (EPE/PEMC), Novi Sad, Serbia, 4–6 September 2012.
48. González, R.; Gubía, E.; López, J.; Marroyo, L. Transformerless single-phase multilevel-based photovoltaic inverter. *IEEE Trans. Ind. Electron.* **2008**, *55*, 2694–2702. [[CrossRef](#)]

49. Jedtberg, H.; Pigazo, A.; Liserre, M.; Buticchi, G. Analysis of the robustness of transformerless PV inverter topologies to the choice of power devices. *IEEE Trans. Power Electron.* **2017**, *32*, 5248–5257. [[CrossRef](#)]
50. Knaup, P. INVERTER. International Patent Application WO/2007/048420, 4 May 2007.
51. Zaragoza, J.; Pou, J.; Ceballos, S.; Robles, E.; Ibáñez, P.; Villate, J.L. A comprehensive study of a hybrid modulation technique for the neutral-point-clamped converter. *IEEE Trans. Ind. Electron.* **2009**, *56*, 294–304. [[CrossRef](#)]
52. Lai, R.S.; Ngo, K.D.T. A PWM Method for Reduction of Switching Loss in a Full-Bridge Inverter. *IEEE Trans. Power Electron.* **1995**, *10*, 326–332.
53. Saridakis, S.; Koutroulis, E.; Blaabjerg, F. Optimization of SiC-based H5 and conergy-NPC transformerless PV inverters. *IEEE J. Emerg. Sel. Top. Power Electron.* **2015**, *3*, 555–567. [[CrossRef](#)]
54. Zhang, L.; Sun, K.; Xing, Y.; Zhao, J. Parallel Operation of Modular Single-Phase Transformerless Grid-Tied PV Inverters with Common DC Bus and AC Bus. *IEEE J. Emerg. Sel. Top. Power Electron.* **2015**, *3*, 858–869. [[CrossRef](#)]
55. Monfared, M.; Golestan, S. Control strategies for single-phase grid integration of small-scale renewable energy sources: A review. *Renew. Sustain. Energy Rev.* **2012**, *16*, 4982–4993. [[CrossRef](#)]
56. González, R.; López, J.; Sanchis, P.; Marroyo, L. Transformerless inverter for single-phase photovoltaic systems. *IEEE Trans. Power Electron.* **2007**, *22*, 693–697. [[CrossRef](#)]
57. Matthias, V.; Frank, G.; Sven, B.; Uwe, H. Method of Converting a Direct Current Voltage from a Source of Direct Current Voltage, More Specifically from a Photovoltaic Couse of Direct Current Voltage, into a Alternating Current Voltage. 2005. Available online: <https://patents.google.com/patent/US7411802B2/en> (accessed on 26 July 2018).
58. Yang, Y.; Blaabjerg, F.; Wang, H. Low-voltage ride-through of single-phase transformerless photovoltaic inverters. *IEEE Trans. Ind. Appl.* **2014**, *50*, 1942–1952. [[CrossRef](#)]
59. Dzung, P.Q.; Dat, D.N.; Anh, N.B.; Hiep, L.C.; Lee, H.H. Design of HERIC inverter for PV systems by using hardware in the loop (HIL) concept. In Proceedings of the 2014 9th IEEE Conference on Industrial Electronics and Applications (ICIEA), Hangzhou, China, 9–11 June 2014.
60. Yang, Y.; Blaabjerg, F.; Wang, H.; Yongheng, Y.; Blaabjerg, F.; Huai, W. Low voltage ride-through of single-phase transformerless photovoltaic inverters. *Energy Convers. Congr. Expo.* **2013**, *50*, 4762–4769.
61. Myrzik, J. *Topologische Untersuchungen zur Anwendung von tief-, hochsetzenden Stellern für Wechselrichter*; Kassel University Press: Kassel, Germany, 2001.
62. Zhang, L.; Sun, K.; Xing, Y.; Xing, M. H6 transformerless full-bridge PV grid-tied inverters. *IEEE Trans. Power Electron.* **2014**, *29*, 1229–1238. [[CrossRef](#)]
63. Yu, W.; Lai, J.S.; Qian, H.; Hutchens, C. High-efficiency MOSFET inverter with H6-type configuration for photovoltaic nonisolated AC-module applications. *IEEE Trans. Power Electron.* **2011**, *26*, 1253–1260. [[CrossRef](#)]
64. Hantschel, J. Inverter Circuit for Extended Input Voltage Range. German Patent DE102006010694A1, 20 September 2007.
65. Coloma, C.J.; Roberto, S.; Taberna, G.; Lopez, J.; Marroyo, P.L.; Sanchis, G.P. Single-Phase Inverter Circuit for Conditioning and Converting dc Electrical Energy into ac Electrical Energy. Available online: <https://patentscope.wipo.int/search/en/detail.jsf?docId=WO2008015298> (accessed on 26 July 2018).
66. Kerekes, T.; Teodorescu, R.; Rodríguez, P.; Vázquez, G.; Aldabas, E. A New high-efficiency single-phase transformerless PV inverter topology. *IEEE Trans. Ind. Electron.* **2011**, *58*, 184–191. [[CrossRef](#)]
67. Roasto, I.; Vinnikov, D.; Vodovozov, V. Simulation and evaluation of control methods for the rolling stock static auxiliary converter based on three-level NPC inverter topology. In Proceedings of the 2009 International Conference on Power Engineering, Energy and Electrical Drives, Lisbon, Portugal, 18–20 March 2009.
68. Oliveira, K.C.; Cavalcanti, M.C.; Afonso, J.L.; Farias, A.M.; Neves, F.A.S. Transformerless photovoltaic systems using neutral point clamped multilevel inverters. In Proceedings of the 2010 IEEE International Symposium on Industrial Electronics, Bari, Italy, 4–7 July 2010.
69. Latha, R.; Bharatiraja, C.; Palanisamy, R.; sudeepbanerji; Dash, S.S. Hysteresis Current Controller based Transformerless Split Inductor-NPC-MLI for Grid Connected PV-System. *Procedia Eng.* **2013**, *64*, 224–233. [[CrossRef](#)]

70. Bharatiraja, C.; Jeevananthan, S.; Latha, R. FPGA based practical implementation of NPC-MLI with SVPWM for an autonomous operation PV system with capacitor balancing. *Int. J. Electr. Power Energy Syst.* **2014**, *61*, 489–509. [[CrossRef](#)]
71. Nabae, A.; Takahashi, I.; Akagi, H. A New Neutral-Point-Clamped PWM Inverter. *IEEE Trans. Ind.* **1981**, *1*, 518–523. [[CrossRef](#)]
72. De Caro, S.; Scimone, T.; Testa, A.; Cacciato, M.; Scarcella, G. A NPC transformerless single phase inverter with inner voltage boosting capability. In Proceedings of the 2014 International Symposium on Power Electronics, Electrical Drives, Automation and Motion (SPEEDAM), Ischia, Italy, 18–20 June 2014.
73. Yuan, L.; Cao, Y.; He, F.; Ma, J.; Chen, Z.; Lu, T.; Zhao, Z. Design and implementation of three-phase two-bridge advanced neutral point clamped three-level photovoltaic inverter. In Proceedings of the 2014 17th International Conference on Electrical Machines and Systems (ICEMS), Hangzhou, China, 22–25 October 2014.
74. William, M. *Inverter Circuits*; General Electric Company: New York, NY, USA, 23 February 1961.
75. Rampinelli, G.A.; Krenzinger, A.; Chenlo Romero, F. Mathematical models for efficiency of inverters used in grid connected photovoltaic systems. *Renew. Sustain. Energy Rev.* **2014**, *34*, 578–587. [[CrossRef](#)]
76. Nayanassiri, D.R.; Vilathgamuwa, D.M.; Maskell, D.L. Half-wave cycloconverter-based photovoltaic microinverter topology with phase-shift power modulation. *IEEE Trans. Power Electron.* **2013**, *28*, 2700–2710. [[CrossRef](#)]
77. Bandara, K.; Sweet, T.; Ekanayake, J. Photovoltaic applications for off-grid electrification using novel multi-level inverter technology with energy storag. *Renew. Energy* **2012**, *37*, 82–88. [[CrossRef](#)]
78. Phanikumar, C.; Agarwal, V. Single phase 9 level grid connected inverter for photovoltaic applications. In Proceedings of the 2013 4th IEEE International Symposium on Power Electronics for Distributed Generation Systems (PEDG), Rogers, AR, USA, 8–11 July 2013.
79. Flores, P.; Dixon, J.; Ortuzar, M.; Carmi, R.; Barriuso, P.; Moran, L. Static Var Compensator and Active Power Filter With Power Injection Capability, Using 27-Level Inverters and Photovoltaic Cells. *IEEE Trans. Ind. Electron.* **2009**, *56*, 130–138. [[CrossRef](#)]
80. Barbosa, P.G.; Braga, H.A.C.; Rodrigues, M.C.B.; Teixeira, E.C. Boost current multilevel inverter and Its application on single-phase grid-connected photovoltaic systems. *IEEE Trans. Power Electron.* **2006**, *21*, 1116–1124. [[CrossRef](#)]
81. Zeng, Z.; Yang, H.; Zhao, R.; Cheng, C. Topologies and control strategies of multi-functional grid-connected inverters for power quality enhancement: A comprehensive review. *Renew. Sust. Energ. Rev.* **2013**, *24*, 223–270. [[CrossRef](#)]
82. Meneses, D.; Blaabjerg, F.; García, Ó.; Cobos, J.A. Review and comparison of step-up transformerless topologies for photovoltaic AC-module application. *IEEE Trans. Power Electron.* **2013**, *28*, 2649–2663. [[CrossRef](#)]
83. Nema, P.; Nema, R.K.; Rangnekar, S. A current and future state of art development of hybrid energy system using wind and PV-solar: A review. *Renew. Sustain. Energy Rev.* **2009**, *13*, 2096–2103. [[CrossRef](#)]
84. Hasanzadeh, A.; Edrington, C.S.; Leonard, J. Reduced switch NPC-based transformerless PV inverter by developed switching pattern. In Proceedings of the 2012 Twenty-Seventh Annual IEEE Applied Power Electronics Conference and Exposition (APEC), Orlando, FL, USA, 5–9 February 2012.
85. Baker, D.M.; Agelidis, V.G.; Nayer, C.V. A comparison of tri-level and bi-level current controlled grid-connected single-phase full-bridge inverters. In Proceedings of the IEEE International Symposium on Industrial Electronics, Guimaraes, Portugal, 7–11 July 1997; pp. 463–468.
86. Rodriguez, J.; Bernet, S.; Steimer, P.K.; Lizama, I.E. A survey on neutral-point-clamped inverters. *IEEE Trans. Ind. Electron.* **2010**, *57*, 2219–2230. [[CrossRef](#)]
87. Araújo, V.; Zacharias, P.; Mallwitz, R. Highly efficient single-phase transformerless inverters for grid-connected photovoltaic systems. *IEEE Trans. Ind. Electron.* **2010**, *57*, 3118–3128. [[CrossRef](#)]
88. Dr, V.M.; Frank, G.; Sven, B.; Uwe, H. Method of Converting A Dc Voltage of A Dc Source, in Particular of a Photovoltaic Dc Source, in an Ac Voltage. European Patent EP1626494, DE10204030912, 24 November 2010.
89. Pimentel, S.P.; Martinez, R.M.M.; Pomilio, J.A. Single-phase distributed generation system based on asymmetrical cascaded multilevel inverter. In Proceedings of the 2009 Brazilian Power Electronics Conference, Bonito-Mato Grosso do Sul, Brazil, 27 September–1 October 2009; pp. 346–353.

90. Gu, Y.; Li, W.; Zhao, Y.; Yang, B.; Li, C.; He, X. Transformerless inverter with virtual DC bus concept for cost-effective grid-connected PV power systems. *IEEE Trans. Power Electron.* **2013**, *28*, 793–805. [[CrossRef](#)]
91. Dominic, J. Comparison and Design of Efficiency Microinverters for Photovoltaic Applications. Master's Thesis, Virginia Tech, Blacksburg, Virginia, 2014.
92. Gu, B.; Dominic, J.; Lai, J.S.; Chen, C.L.; Labella, T.; Chen, B. High reliability and efficiency single-phase transformerless inverter for grid-connected photovoltaic systems. *IEEE Trans. Power Electron.* **2013**, *28*, 2235–2245. [[CrossRef](#)]
93. Wang, J.; Ji, B.; Zhao, J.; Yu, J. From H4, H5 to H6 Standardization of full-bridge single phase photovoltaic inverter topologies without ground leakage current issue. In Proceedings of the 2012 IEEE Energy Conversion Congress and Exposition, Raleigh, NC, USA, 15–20 September 2012; pp. 2419–2425.
94. Kjær, S.B. *Design and Control of an Inverter for Photovoltaic Applications*; Aalborg Universitet: Aalborg, Denmark, 2005.
95. Junior, L.G.; De Brito, M.A.G.; Sampaio, L.P.; Canesin, C.A. Single stage converters for low power stand-alone and grid-connected PV systems. In Proceedings of the ISIE 2011: 2011 IEEE International Symposium on Industrial Electronics, Gdansk, Poland, 27–30 June 2011.
96. Cáceres, R.O.; Barbi, I. A boost DC-AC converter: Analysis, design, and experimentation. *IEEE Trans. Power Electron.* **1999**, *14*, 134–141.
97. Funabiki, S.; Tanaka, T.; Nishi, T. A new buck-boost-operation-based sinusoidal inverter circuit. In Proceedings of the 2002 IEEE 33rd Annual IEEE Power Electronics Specialists Conference. Proceedings (Cat. No.02CH37289), Cairns, Australia, 23–27 June 2002.
98. Vazquez, N.; Almazan, J.; Alvarez, J.; Aguilar, C.; Arau, J. Analysis and experimental study of the buck, boost and buck-boost inverters. In Proceedings of the 30th Annual IEEE Power Electronics Specialists Conference. Record. (Cat. No. 99CH36321), Charleston, SC, USA, 27 June–1 July 1999.
99. Wang, C.M. A novel single-stage full-bridge buck-boost inverter. In Proceedings of the Eighteenth Annual IEEE Applied Power Electronics Conference and Exposition, 2003 (APEC'03), Miami Beach, FL, USA, 9–13 February 2003.
100. Jain, S.; Agarwal, V. A Single-Stage Grid Connected Inverter Topology for Solar PV Systems With Maximum Power Point Tracking. *IEEE Trans. Power Electron.* **2007**, *22*, 1928–1940. [[CrossRef](#)]
101. Blaabjerg, F.; Teodorescu, R.; Liserre, M.; Timbus, A.V. Overview of control and grid synchronization for distributed power generation systems. *IEEE Trans. Ind. Electron.* **2006**, *53*, 1398–1409. [[CrossRef](#)]
102. Bautista, B.; Lázaro Blanco, A. *Problemas de Electrónica de Potencia*; Pearson Prentice Hall: Madrid, Spain, 2007.
103. Svensson, J. Synchronisation methods for grid-connected voltage source converters. *IEE Proc.-Gener. Transm. Distrib.* **2001**, *148*, 229–235. [[CrossRef](#)]
104. Mahela, O.P.; Shaik, A.G. Comprehensive overview of grid interfaced solar photovoltaic systems. *Renew. Sust. Energ. Rev.* **2017**, *68*, 316–332. [[CrossRef](#)]

